Theory of saturation spectroscopy including effects of level degeneracy

C. Feuillade* and P. R. Berman
Physics Department, New York University, 4 Washington Place, New York, New York 10003
(Received 28 March 1983)

A theory of saturation spectroscopy is developed which accounts for effects of level degeneracy. The theory can be applied to those situations in which a pump laser field of arbitrary strength and polarization acts between two manifolds of degenerate or nearly degenerate atomic levels, while a probe laser field of arbitrary strength and polarization acts between a coupled manifold of levels. As such, this theory of "three-level" systems could, in principle, include effects arising from level degeneracy, optical pumping, atomic motion, transient laser fields, different polarizations and strengths for pump and probe fields, and atomic transit across the laser fields. The present calculation, however, is limited to a study of optical pumping and field polarization effects for pump fields of arbitrary strength and weak probe fields interacting with a single velocity subclass of atoms. Probe absorption line shapes clearly display the effects of pump-field strength (Rabi splittings), pump-field polarization (positions and number of Rabi-split resonance peaks), pump-field detuning (positions of resonance peaks), and optical pumping (relative strengths of the resonance peaks). The calculation is carried out with the use of an irreducible tensor basis for the atomic density matrix although a standard (m-basis) calculation is included in an appendix.

I. INTRODUCTION

Over the past 15 years, laser saturation spectroscopy has become an accepted method for obtaining Doppler-free spectra of atomic and molecular vapors. The three-level system (see Fig. 1) is typical of the level scheme employed in a laser spectroscopy experiment. A "pump" laser acting on the b-c transition selectively excites a velocity subclass of atoms. A "probe" laser acting on the coupled c-d transition interacts with this excited velocity subclass only; consequently the linewidth of the probe absorption line profile is determined by the natural rather than the Doppler width associated with the transition. Owing to its relative importance as a prototype system, the three-level configuration has been of extensive theoretical[1-38] and experimental[1,12,14,19,29,35,39-46] interest.

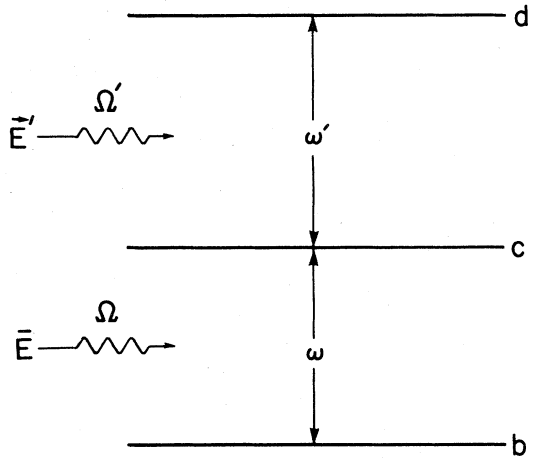

FIG. 1. A schematic representation of a three-level system used in laser spectroscopy experiments.

In many situations of practical importance, the actual level structure encountered in a given problem cannot be adequately represented by a "three-level" approximation. For example, the often used three-level system in Na ($3S \rightarrow 3P \rightarrow 4D$) is actually composed of 72 levels. Of these 72 levels, the number that enters into a given saturation spectroscopy experiment depends on the laser bandwidth, laser polarization, and the tuning range of the pump and probe laser fields that are used. In formulating a complete theory of saturation spectroscopy for this multilevel system, one must solve the equations of motion for the density-matrix elements characterizing the system. If all 72 levels enter, one is faced with 5184 density-matrix elements for *each* velocity subclass of atoms. The problem can be substantially simplified if narrow-band lasers are used such that the laser-induced transitions can be assumed to occur between specific hyperfine states of the $3S$, $3P$, and $4D$ manifolds.

In this paper, we develop a general formalism that can be used to solve problems involving three-level systems with magnetic degeneracy. The type of level scheme under consideration is shown in Fig. 2. There are three manifolds of levels, labeled 1, 2, and 3, respectively. Within a given manifold, the levels (labeled by Roman letters) are nearly degenerate and could represent for example, different hyperfine levels within a given fine-structure multiplet. Each level labeled by a Roman letter is characterized by a total angular momentum quantum number F and is *itself* degenerate, containing $(2F+1)$ magnetic sublevels. A pump laser field of arbitrary polarization acts between manifolds 1 and 2, while a probe laser field (which, in principle, can be of arbitrary strength) acts

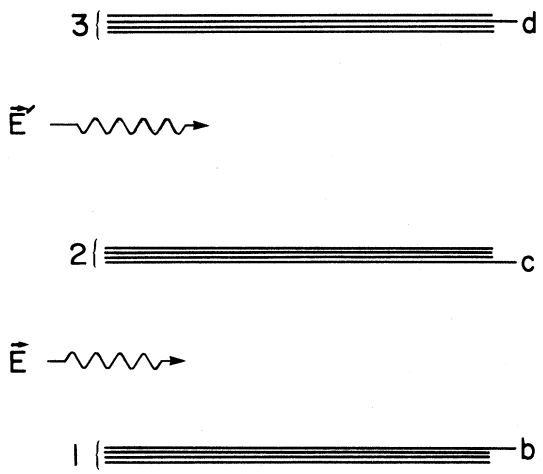

FIG. 2. Level scheme of Fig. 1 generalized to allow for level degeneracy.

between manifolds 2 and 3. The frequency separations between the manifolds is such that the pump field drives the 1-2 manifold only and the probe field the 2-3 manifold only.

Using irreducible tensor techniques (which will be extremely useful when relaxation processes are included), we formulate the theory in a way that can incorporate effects arising from atomic motion, optical pumping (resulting from spontaneous emission), transient laser fields, and finite transit times of the atoms in the laser field. Several other treatments of magnetic degeneracy effects in three-level systems exist[1,6,12,14,22,24,34,38] but none, to our knowledge, provides the type of generality to be presented below. As an application of the formalism, we calculate the steady-state probe absorption line shape when a strong pump field acts between two degenerate sets of levels of the 1-2 manifold and a weak probe field between two degenerate sets of levels of the 2-3 manifold. The calculation is performed for a single velocity subclass of atoms; that is, no integration over the atomic velocity distribution is carried out. As such, the calculation, at its present stage, is applicable to laser fields interacting with an atomic beam rather than to laser fields interacting with an atomic vapor in a cell. Optical-pumping effects are included. The resultant line shapes will be seen to be strongly dependent on the pump-field strength, polarization, and detuning, as well as on any optical-pumping processes that may be occurring.

The paper is organized as follows. In Secs. II–IV some properties of irreducible tensor operators are reviewed and the equations of motion for density-matrix elements, appropriate to the atom-field interaction under consideration, are obtained. In Sec. V, a steady-state solution, applicable to the strong-pump-field, weak-probe-field limit is derived in a manner analogous to that employed in treating three-level nondegenerate systems. Probe absorption line shapes for specific values of the pump-field strength, detuning, and polarization are presented in Sec. VI, along with the modifications arising from optical pumping. There are also two appendixes containing somewhat complementary calculations. In Appendix A, the problem is recast and solved in the standard (m-basis) representation. This representation is particularly useful in obtaining steady-state line shapes when the pump and probe fields are either linearly or circularly (but not elliptically) polarized and when there is no collisional relaxation. In Appendix B, we use a dressed-atom picture to obtain predictions for the positions of resonances that appear in the (weak) probe absorption line shape when a strong pump field of arbitrary polarization acts between manifolds 1 and 2.

II. THE LIOUVILLE EXPANSION

The method used here to derive the equations which describe the interaction of laser radiation with an atomic system involves a Liouville expansion of the density-matrix equation of motion for the system; a procedure that has been discussed by Fano.[47,48] The ensemble behavior of the atoms is described by the density matrix ρ, which is expanded in terms of a complete set of operators O spanning the Hilbert space of the system. These operators are chosen so that any arbitrary pair of them, say O_I and O_J, obey the orthonormality condition

$$\mathrm{Tr}(O_I^\dagger O_J)=\delta_{IJ} \tag{1}$$

so that if ρ is written

$$\rho=\sum_I \rho_I O_I \ , \tag{2}$$

then it may be easily shown

$$\rho_I=\mathrm{Tr}(O_I^\dagger \rho) \ . \tag{3}$$

The corresponding expansion of the Schrödinger equation for the density matrix,

$$\dot{\rho}=-\frac{i}{\hbar}(H\rho-\rho H) \ , \tag{4}$$

where H is a semiclassical Hamiltonian which includes the perturbations due to the incident laser radiation, leads to a set of coupled first-order differential equations for the time-dependent coefficients ρ_I in Eq. (2),

$$\dot{\rho}_I=\sum_J L_{IJ}\rho_J \ , \tag{5}$$

where the component of the "Liouville matrix" L_{IJ} is related to the Hamiltonian H and to the operators O by the expression

$$L_{IJ}=\frac{i}{\hbar}\mathrm{Tr}(H[O_I^\dagger,O_J]) \ . \tag{6}$$

For nondegenerate two- and three-level systems, the operators O take the form of sets of two- and three-dimensional Lie matrices, respectively.[49,50] The equations derived using these matrices have been applied to numerous problems in laser and molecular physics and are well described in textbooks and review articles.[51–53]

In the case of degenerate level systems, it is convenient

to expand the density matrix in terms of a set of spherical tensor operators O, which span the degenerate space of the atomic energy levels between which pumping takes place. This method has been discussed by Omont,[54] and has been used previously to describe single- and double-resonant radiative processes between molecular rotational energy levels.[55,56] In this case, the tensor operators are constructed by forming Clebsch-Gordan expansions of projection operators between the hyperfine energy eigenstates $|F,m_F\rangle$ of the atomic system. Therefore, if we consider two hyperfine states F_i,F_j of the system, we may define

$$O_Q^K(i,j)=\sum_{m,n}(-1)^{F_j-n}\langle K,Q\,|\,F_i,m;F_j,\bar{n}\rangle \times|F_i,m\rangle\langle F_j,n|\ , \tag{7a}$$

$$[O_Q^K(i,j)]^\dagger=(-1)^{F_j-F_i+Q}O_{\bar{Q}}^K(j,i)\ , \tag{7b}$$

where the factor $(-1)^{F_j}$ indicates a choice of phase, and $\bar{n}\equiv -n$; $\bar{Q}\equiv -Q$. When evaluated in the energy state representation, this operator may also be thought of as a vector-coupled combination of density-matrix elements. Thus expanding ρ in terms of the members of O, cf. Eq. (2),

$$\rho=\sum_{K,Q,i,j}\rho_Q^K(i,j)O_Q^K(i,j) \tag{8}$$

gives

$$\rho_Q^K(i,j)=\sum_{m,n}(-1)^{F_j-n}\langle K,Q\,|\,F_i,m\,;F_j,\bar{n}\rangle\rho_{mn}(i,j)\ , \tag{9}$$

where $\rho_{mn}(i,j)$ is the matrix element of the density matrix between the energy eigenstates $|F_i,m\rangle$ and $|F_j,n\rangle$. If $i=j$, then the quantities defined in Eq. (9) are related to properties of the state F_i alone. These could be the total population of the state, or the alignment or orientation among its degenerate components, depending upon the value of K. If $K=Q=0$, then we have quite simply

$$\rho_0^0(i,i)=\sum_m(-1)^{F_i-n}\langle 0,0\,|\,F_i,m\,;F_i,\bar{m}\rangle\rho_{mm}(i,i) =\frac{N(F_i)}{\sqrt{2F_i+1}}\ , \tag{10}$$

where $N(F_i)$ is the total population of the state F_i. If $i\neq j$ then the quantities defined by Eq. (9) are tensor multipoles of different ranks describing the coherent coupling of the two states. For example, the first-ranked tensors $\rho_Q^1(i,j)$, for two atomic states i and j which are dipole connected, are directly related to the dielectric polarization induced in the atom by an applied field coupling the two states.[55]

We see that a Liouville expansion of the density-matrix equation of motion, in terms of the tensors defined by Eq. (9), leads to a set of equations involving quantities which are closely related to physical properties of the atomic system. These are given by the expression, cf. Eqs. (5) and (6),

$$\dot{\rho}_Q^K(i,j)=\sum_{K',Q',r,s}L_{QQ'}^{KK'}(i,j;r,s)\rho_{Q'}^{K'}(r,s)\ , \tag{11}$$

where

$$L_{QQ'}^{KK'}(i,j;r,s)=\frac{i}{\hbar}\mathrm{Tr}\{H[[O_Q^K(i,j)]^\dagger,O_{Q'}^{K'}(r,s)]\}\ . \tag{12}$$

The values of K',Q',r,s entering the sum in Eq. (11) reflect the various multipoles and intermediate states that are coupled into the problem by the external fields. An explicit evaluation of the elements of the Liouville matrix, as in Eq. (12), will be given in Sec. IV.

III. THE HAMILTONIAN

In this section we will show how the Hamiltonian for a two-level nondegenerate system may be expressed in a rotating frame, and then demonstrate that the resulting expression may be readily adapted to the degenerate case. The Hamiltonian which appears in Eq. (4) may be written

$$H=H_0+U(t)\ , \tag{13}$$

where the time-independent part H_0 is the unperturbed atomic Hamiltonian and $U(t)$ describes the time-dependent perturbations on the system due to the incident laser field. We will perform the Liouville expansion of Eq. (4) following transformation into a frame rotating at the incident field frequency and after the application of the rotating-wave approximation.[55] Let us denote the transformed Hamiltonian by $\tilde{H}$. The terms which will appear in the equations as a result of commutation of the operators O with $\tilde{H}_0$ in Eq. (12), will describe free precession of the system if solved for zero field.[56] Those appearing due to $\tilde{U}$ describe the coherent radiative coupling of the system. We will now derive an expression for $\tilde{U}$ in terms of the operators defined by Eq. (7), which may be directly applied in the derivation of the radiative equations from Eqs. (11) and (12).

The atom-field interaction may be written

$$U(t)=-\vec{\mathrm{D}}\cdot\vec{\mathrm{E}}(t)\ , \tag{14}$$

where $\vec{\mathrm{D}}$ is the dipole moment operator of the atomic system and $\vec{\mathrm{E}}(t)$ represents the time-dependent electric field of the laser (the following analysis applies equally to magnetic dipole transitions). In the atomic rest frame, it is convenient to write $\vec{\mathrm{E}}$ as

$$\vec{\mathrm{E}}(t)=\tfrac{1}{2}(\vec{\mathscr{E}}e^{i\Omega t}+\vec{\mathscr{E}}^{\,*}e^{-i\Omega t})\ , \tag{15}$$

where $\vec{\mathscr{E}}$ (a complex variable) represents a state of arbitrary polarization and Ω is the frequency of the radiation including the Doppler shift. The first step in the derivation is to consider matrix elements of $U(t)$, as defined by Eqs. (14) and (15) between two nondegenerate states of an atom, which for our purposes here we may define simply as $|i\rangle$ and $|j\rangle$. Then, U may be expanded

$$\underline{U}(t)=-\frac{1}{2}\begin{bmatrix}0 & \vec{\mathrm{D}}_{ij}\cdot\vec{\mathscr{E}}e^{i\Omega t}\\ \vec{\mathrm{D}}_{ji}\cdot\vec{\mathscr{E}}^{\,*}e^{-i\Omega t} & 0\end{bmatrix} -\frac{1}{2}\begin{bmatrix}0 & \vec{\mathrm{D}}_{ij}\cdot\vec{\mathscr{E}}^{\,*}e^{-i\Omega t}\\ \vec{\mathrm{D}}_{ji}\cdot\vec{\mathscr{E}}e^{i\Omega t} & 0\end{bmatrix}, \tag{16}$$

where $\vec{D}_{ij} \equiv \langle i | \vec{D} | j \rangle$ and $\vec{D}_{ji} \equiv \langle j | \vec{D} | i \rangle$ are dipole matrix elements between the two states. Now $\underline{U}$ is taken into the rotating frame by the matrix transformation

$$\underline{\tilde{U}} = \exp\left[\frac{i\underline{T}t}{\hbar}\right] \underline{U} \exp\left[\frac{-i\underline{T}t}{\hbar}\right], \tag{17}$$

where

$$\underline{T} = \frac{\hbar\Omega}{2}\begin{bmatrix} -1 & 0 \\ 0 & 1 \end{bmatrix} \tag{18}$$

and the tilde indicates the interaction representation of the applied field. Explicitly the transformed matrix $\underline{\tilde{U}}$ is

$$\underline{\tilde{U}} = -\frac{1}{2}\begin{bmatrix} 0 & \vec{D}_{ij}\cdot\vec{\mathscr{E}} \\ \vec{D}_{ij}\cdot\vec{\mathscr{E}} & 0 \end{bmatrix} - \frac{1}{2}\begin{bmatrix} 0 & \vec{D}_{ij}\cdot\vec{\mathscr{E}}^{*}e^{-2i\Omega t} \\ \vec{D}_{ji}\cdot\vec{\mathscr{E}}e^{2i\Omega t} & 0 \end{bmatrix}. \tag{19}$$

Making the rotating-wave approximation[57] involves neglecting the terms in the second matrix on the right-hand side (rhs) of Eq. (19) which are varying quickly compared with the Rabi frequency. Under conditions typically encountered in laser spectroscopy experiments, these may be reasonably neglected since they produce only a small perturbative effect giving rise to the Bloch-Seigert shift. The time evolution of the atomic system is dominated by the terms in the first matrix on the rhs.

When we come to consider matrix elements of $U(t)$ between two degenerate energy levels of an atom, we will obtain a form for $\underline{\tilde{U}}$ analogous to that in (19), with each matrix element in Eq. (19) replaced by a *matrix* which couples one set of degenerate levels to another. In order to derive $\underline{\tilde{U}}$ for a pair of degenerate hyperfine states F_i, F_j coupled by an incident radiation field, we express the dipole operator $\vec{D}$ in terms of the first-ranked basis tensor operators $O_Q^1(i,j)$ defined in Eq. (7).

Noting that,

$$\vec{D}\cdot\vec{\mathscr{E}} = \sum_{q=-1}^{1} (-1)^q D_q^1 \epsilon_{\bar{q}}^1 |\vec{\mathscr{E}}|, \tag{20}$$

where D_q^1 form the components of an irreducible tensor of rank 1 and the ϵ_q^1 are defined by

$$\epsilon_{\pm1} = \mp\frac{1}{\sqrt{2}}(\epsilon_x \pm i\epsilon_y), \quad \epsilon_0 = \epsilon_z, \tag{21}$$

and $\hat{\epsilon} = (\epsilon_x, \epsilon_y, \epsilon_z)$ is the complex field polarization vector defined by

$$\vec{\mathscr{E}} = \hat{\epsilon}\,|\vec{\mathscr{E}}|, \tag{22}$$

we can rewrite the atom-field interaction as

$$\tilde{U} = -\sum_{q=-1}^{1} (-1)^q [G_{ij}\epsilon_{\bar{q}} O_q^1(i,j) + (-1)^{F_j - F_i + q} G_{ij} (\epsilon_{\bar{q}})^* O_{\bar{q}}^1(j,i)], \tag{23}$$

where

$$G_{ij} = \frac{1}{(2\sqrt{3})}\langle F_i || D^1 || F_j \rangle |\vec{\mathscr{E}}| \tag{24}$$

has been taken as real by an appropriate choice of phase. In writing Eq. (23), we have adopted the convention that state F_i has a lower energy than state F_j; were the situation reversed, there would be a corresponding reversal in the coefficients [i.e., $\epsilon_q^* \leftrightarrow (-1)^q \epsilon_{\bar{q}}$] multiplying the basis operators.

IV. DERIVING THE LIOUVILLE EQUATIONS

The results of Sec. III can be generalized to allow one to obtain the Liouville equation for a multilevel atom inteacting with one or more radiation fields. Each atomic level i is characterized by total angular momentum F_i and is $(2F_i+1)$-fold degenerate. Each radiation field of amplitude $|\vec{\mathscr{E}}_{ij}|$, polarization $\hat{\epsilon}(i,j)$, and frequency Ω_{ij} is assumed to be nearly resonant with the i-j transition. While equations of the type of Eq. (23) are easily written for an arbitrary multilevel system of the type described, we immediately restrict our discussion to the level scheme of Fig. 3. In this scheme, levels b and c are coupled by the field $\vec{\mathscr{E}}_{bc}$, levels c and d by the field $\vec{\mathscr{E}}_{cd}$. Level a is *not* coupled by the fields and acts as a sink only; consequently, off-diagonal density-matrix elements of the form $\rho_Q^K(a,j)$ ($j = b$, c, or d) can be neglected.

A. The radiation coupling terms

It is again convenient to adopt a field interaction representation. In analogy with Eqs. (17) and (18), one can introduce a matrix $\exp(i\underline{T}t/\hbar)$ that generates the appropriate transition to the rotating frame. For the level scheme chosen, $\underline{T}$ is a diagonal matrix with elements

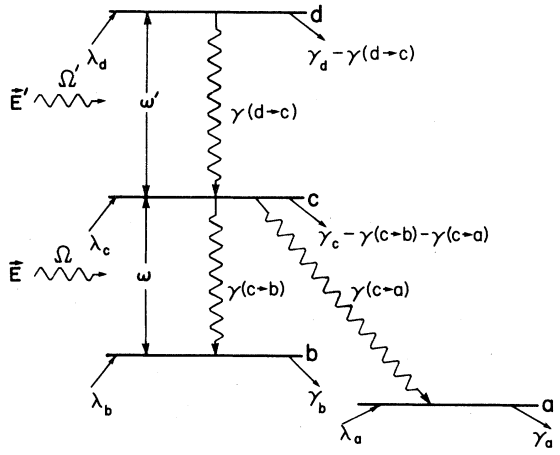

FIG. 3. Specific level scheme considered in this work. Each level α ($\alpha = a,b,c,d$) is characterized by an angular momentum F_α and is $(2F_\alpha+1)$-fold degenerate.

$$T_{aa}=T_{bb}=-\tfrac{1}{2}\hbar(\Omega_{bc}+\Omega_{cd})\ ,$$
$$T_{cc}=\tfrac{1}{2}\hbar(\Omega_{bc}-\Omega_{cd}),\quad T_{dd}=\tfrac{1}{2}\hbar(\Omega_{bc}+\Omega_{cd})\ . \tag{25}$$

In the rotating frame, the Liouville equation may be written

$$\dot{\rho}^K_Q(f,g)=-i(T_{gg}-T_{ff})\rho^K_Q(f,g)+\sum_{K',Q',r,s}\tilde{L}^{KK'}_{QQ'}(f,g;r,s)\rho^{K'}_{Q'}(r,s)\ , \tag{26}$$

where the first term on the rhs gives the precession at the field frequency. We have omitted writing the tildes on the ρ^K_Q terms, but the field interaction representation is to be understood.

The atom-field interaction Hamiltonian is a direct generalization of Eq. (23) and may be written

$$\tilde{U}=-\sum_{q=-1}^{1}\sum_{i,j=b,c;c,d}(-1)^q G_{ij}\{\epsilon_{\bar{q}}(i,j)O^1_q(i,j)+(-1)^{F_j-F_i+q}[\epsilon_{\bar{q}}(i,j)]^*O^1_q(j,i)\}\ , \tag{27}$$

where

$$G_{ij}=\frac{1}{(2\sqrt{3})}\langle F_i||D^1||F_j\rangle\,|\,\vec{\mathscr{E}}_{ij}\,|=G^*_{ij}\ . \tag{28}$$

By a direct application of Eqs. (7) and (12) one can easily calculate

$$\begin{aligned}[\tilde{L}^{KK'}_{QQ'}(f,g;r,s)]_{\text{atom-field}}&=\frac{i}{\hbar}[3(2K'+1)]^{1/2}(-1)^{F_f+F_g+K+1}\\&\times\sum_{q=-1}^{1}(-1)^q\sum_{i,j=b,c;c,d}\Bigg[G_{ij}\epsilon_{\bar{q}}(i,j)\Bigg(\langle K,Q\,|\,K',Q';1,q\rangle\begin{Bmatrix}K&K'&1\\F_s&F_g&F_f\end{Bmatrix}\delta_{fr}\delta_{is}\delta_{jg}\\&\qquad-\langle K,Q\,|\,1,q;K',Q'\rangle\begin{Bmatrix}K&K'&1\\F_r&F_f&F_s\end{Bmatrix}\delta_{gs}\delta_{if}\delta_{jr}\Bigg)\\&+(-1)^{F_j-F_i+q}G_{ij}[\epsilon_{\bar{q}}(i,j)]^*\Bigg(\langle K,Q\,|\,K',Q';1,\bar{q}\rangle\begin{Bmatrix}K&K'&1\\F_s&F_g&F_f\end{Bmatrix}\delta_{fr}\delta_{js}\delta_{ig}\\&\qquad-\langle K,Q\,|\,1,\bar{q};K',Q'\rangle\begin{Bmatrix}K&K'&1\\F_r&F_f&F_s\end{Bmatrix}\delta_{gs}\delta_{jf}\delta_{ir}\Bigg)\Bigg]\ .\end{aligned} \tag{29}$$

B. The "free-precession" terms

The free atomic Hamiltonian $\tilde{H}_0$ may be written as

$$\tilde{H}_0=\sum_i E_i\sqrt{2F_i+1}\,O^0_0(i,i) \tag{30}$$

and it follows immediately from Eqs. (7) and (12) that

$$\tilde{L}^{KK'}_{QQ'}(f,g;r,s)]_{H_0}=i\omega_{gf}\delta_{fr}\delta_{gs}\delta_{KK'}\delta_{QQ'}\ , \tag{31}$$

where

$$\omega_{gf}=(E_g-E_f)/\hbar\ . \tag{31'}$$

Note that these free-precession terms will combine with those appearing in Eq. (26) to give a frequency detuning precession for the off-diagonal terms.

C. The spontaneous decay terms

In the Introduction, it was stated that this article would be concerned with atomic systems in which spontaneous relaxation was the dominant damping process. The calculation of spontaneous decay rates between degenerate atomic states using the method of the quantized radiation field is, of course, well known.[58] The corresponding rates for decay between spherical tensor density-matrix elements have been presented by Dumont[59] and Ducloy.[60] We shall briefly summarize the results which are relevant to the system under consideration here.

Spontaneous emission leads to decay terms of the form

$$[\tilde{L}^{KK'}_{QQ'}(f,g;r,s)]_{\text{decay}}=-\gamma_{fg}\delta_{fr}\delta_{gs}\delta_{KK'}\delta_{QQ'}\ , \tag{32}$$

where

$$\gamma_{fg}=\tfrac{1}{2}(\gamma_f+\gamma_g)\ , \tag{33}$$
$$\gamma_f=\sum_i\gamma(f\to i)\ , \tag{34}$$

and $\gamma(f\to i)$ is the spontaneous decay rate from state f to state i. The sum in Eq. (34) is over all states i to which state f decays.

There can also be an "in" term resulting from states being populated by spontaneous decay from higher-lying states. The Liouvillian matrix elements for this contributione are

$$[\tilde{L}^{KK'}_{QQ'}(f,g;r,s)]_{\text{in}}=\gamma^K(r\to f)\delta_{fg}\delta_{rs}\delta_{KK'}\delta_{QQ'}\ , \tag{35}$$

where

$$\gamma^K(r\to f)=(-1)^{F_r+F_f+K+1}(2F_r+1)\times\begin{Bmatrix}F_r & F_r & K\\ F_f & F_f & 1\end{Bmatrix}\gamma(r\to f)\ . \tag{36}$$

We note that K and Q are conserved in all these decay processes.

D. Incoherent pumping and transit-time effects

It is often convenient to consider the system as open rather than closed. Additional loss terms can be simply included in the γ_i terms introduced above. Source terms, representing some incoherent injection of atoms into the system can be included by adding a term of the form

$$\lambda_r^0\delta_{fr}\delta_{gs}\delta_{KK'}\delta_{QQ'}\delta_{K0}\delta_{Q0} \tag{37}$$

to the rhs of Eq. (26). It should be noted that λ_r^0 is a source term for $\rho_0^0(r,r)$; the corresponding source term for the population is $(2F_r+1)^{1/2}\lambda_r^0$.

E. Equations for density-matrix elements

Equations (26), (29), (31), (32), (35), and (37) may now be combined. Before doing so, it is convenient to simplify the notation somewhat. We define

$$G=\frac{G_{bc}}{\hbar},\quad G'=\frac{G_{cd}}{\hbar}\ ,$$
$$\hat{\epsilon}=\hat{\epsilon}(b,c),\quad \hat{\epsilon}'=\hat{\epsilon}(c,d)\ , \tag{38}$$
$$\Omega=\Omega_{cb},\quad \Omega'=\Omega_{dc}\ ,$$
$$\omega=\omega_{cb},\quad \omega'=\omega_{dc}\ ,$$

so that unprimed variables refer to the b-c transition and primed ones to the c-d transition. Moreover, we define a column vector $\vec{u}$ with elements

$$\vec{u}=(\vec{\rho}(a),\vec{\rho}(b),\vec{\rho}(b,c),\vec{\rho}(c,b),\vec{\rho}(c),\vec{\rho}(c,d),\vec{\rho}(d,c),\vec{\rho}(b,d),\vec{\rho}(d,b),\vec{\rho}(d))\ , \tag{39}$$

where, for brevity, we have defined

$$\vec{\rho}(i)=\vec{\rho}(i,i)\ . \tag{40}$$

Note that each "element" in vector $\vec{u}$ is itself a vector containing components having the various allowed values for K and Q, determined by the multipole structure of the levels involved. Similarly, the incoherent pump matrix may be written

$$\vec{\lambda}=(\vec{\lambda}(a),\vec{\lambda}(b),0,0,\vec{\lambda}(c),0,0,0,0,\vec{\lambda}(d)) \tag{41}$$

and the Liouville equation takes the vector form

$$\dot{\vec{u}}=\underline{\tilde{L}}\vec{u}+\vec{\lambda}\ , \tag{42}$$

where $\underline{\tilde{L}}$ has contributions from the atom-field interaction and the free-precession and spontaneous-decay terms. Moreover, the field-precession terms $\hbar^{-1}(T_{ff}-T_{gg})$ appearing in Eq. (26) have been incorporated into $\underline{\tilde{L}}$. Explicitly, one finds

$$\dot{\rho}_Q^K(a)=-\gamma_a\rho_Q^K(a)+\gamma^K(c\to a)\rho_Q^K(c)+\lambda_a^0\delta_{K0}\delta_{Q0}\ , \tag{43}$$

$$\dot{\rho}_Q^K(b)=-\gamma_b\rho_Q^K(b)+\gamma^K(c\to b)\rho_Q^K(c)+\lambda_b^0\delta_{K0}\delta_{Q0}+iG\sum_{K',Q',q}[(-1)^{F_b+F_c}(\epsilon_{\bar{q}})^*\Lambda_{cbb}^{KK'\bar{q}}\rho_{Q'}^{K'}(b,c)-(-1)^{2F_b+q+K'-K+1}\epsilon_{\bar{q}}\Lambda_{cbb}^{KK'q}\rho_{Q'}^{K'}(c,b)]\ , \tag{44}$$

$$\dot{\rho}_Q^K(c)=-\gamma_c\rho_Q^K(c)+\gamma^K(d\to c)\rho_Q^K(d)+\lambda_c^0\delta_{K0}\delta_{Q0}+iG\sum_q[(-1)^{2F_c+q}\epsilon_{\bar{q}}\Lambda_{bcc}^{KK'q}\rho_{Q'}^{K'}(c,b)-(-1)^{F_b+F_c+K'-K+1}(\epsilon_{\bar{q}})^*\Lambda_{bcc}^{KK'\bar{q}}\rho_{Q'}^{K'}(b,c)]+iG'\sum_q[(-1)^{F_c+F_d}(\epsilon'_{\bar{q}})^*\Lambda_{dcc}^{KK'\bar{q}}\rho_{Q'}^{K'}(c,d)-(-1)^{2F_c+q+K'-K+1}\epsilon'_{\bar{q}}\Lambda_{dcc}^{KK'q}\rho_{Q'}^{K'}(d,c)]\ , \tag{45}$$

$$\dot{\rho}_Q^K(d)=-\gamma_d\rho_Q^K(d)+\lambda_d^0\delta_{K0}\delta_{Q0}+iG'\sum_q[(-1)^{2F_d+q}\epsilon'_{\bar{q}}\Lambda_{cdd}^{KK'q}\rho_{Q'}^{K'}(d,c)-(-1)^{F_c+F_d+K'-K+1}(\epsilon'_{\bar{q}})^*\Lambda_{cdd}^{KK'\bar{q}}\rho_{Q'}^{K'}(c,d)]\ , \tag{46}$$

$$\dot{\rho}_Q^K(b,c)=-(\gamma_{bc}+i\Delta)\rho_Q^K(b,c)+iG\sum_q\{(-1)^{F_b+F_c+q}\epsilon_{\bar{q}}[\Lambda_{bcb}^{KK'q}\rho_{Q'}^{K'}(b)-(-1)^{K'-K+1}\Lambda_{cbc}^{KK'q}\rho_{Q'}^{K'}(c)]\}+iG'\sum_q[(-1)^{F_b+F_d}(\epsilon'_{\bar{q}})^*\Lambda_{dcb}^{KK'\bar{q}}\rho_{Q'}^{K'}(b,d)]\ , \tag{47}$$

$$\dot{\rho}_Q^K(c,d)=-(\gamma_{cd}+i\Delta')\rho_Q^K(c,d)+iG'\sum_q\{(-1)^{F_c+F_d+q}\epsilon'_{\bar{q}}[\Lambda_{cdc}^{KK'q}\rho_{Q'}^{K'}(c)-(-1)^{K'-K+1}\Lambda_{dcd}^{KK'q}\rho_{Q'}^{K'}(d)]\}$$

$$+iG\sum_q[(-1)^{F_b+F_d+K'-K}(\epsilon_{\bar{q}})^*\Lambda_{bcd}^{KK'\bar{q}}\rho_{Q'}^{K'}(b,d)]\ , \tag{48}$$

$$\dot{\rho}_Q^K(b,d)=-[\gamma_{bd}+i(\Delta+\Delta')]\rho_Q^K(b,d)+i\sum_q(-1)^{F_b+F_d+q}[(-1)^{K'-K}G\epsilon_{\bar{q}}\Lambda_{cbd}^{KK'q}\rho_{Q'}^{K'}(c,d)+G'\epsilon'_{\bar{q}}\Lambda_{cdb}^{KK'q}\rho_{Q'}^{K'}(b,c)]\ , \tag{49}$$

$$\rho_Q^K(g,f)=(-1)^{F_f-F_g+Q}\rho_{\bar{Q}}^K(f,g)\ , \tag{50}$$

where

$$\Delta=\Omega-\omega,\ \Delta'=\Omega'-\omega'\ , \tag{51}$$

and

$$\Lambda_{fgr}^{KK'q}=(-1)^{K+1}[3(2K'+1)]^{1/2}\times\langle K,Q\,|\,K',Q';1q\rangle\begin{Bmatrix}K & K' & 1\\ F_f & F_g & F_r\end{Bmatrix}\ . \tag{52}$$

These equations have the same basic structure as those for the nondegenerate case.[2–13]

V. STEADY-STATE SOLUTIONS

In this section, we describe a procedure for obtaining the steady-state solutions of Eq. (42) and calculate the upper-state population as a function of the strength and detuning of the pump field, assuming that the probe field is weak enough to be treated in lowest-order perturbation theory.

Before outlining the perturbation solution, it is convenient to perform some algebraic manipulations on Eqs. (43) and (46). The steady-state equations for the density-matrix elements may be written as

$$\underline{\tilde{L}}\,\vec{u}+\vec{\lambda}=\vec{0}\ . \tag{53}$$

From Eq. (43), one immediately notes that the steady-state solution for $\rho_Q^K(a)$ is

$$\rho_Q^K(a)=\frac{\lambda_a^0\delta_{K0}\delta_{Q0}}{\gamma_a}+\frac{\gamma^K(c\to a)\rho_Q^K(c)}{\gamma_a}\ . \tag{54}$$

With this solution, we can omit $\vec{\rho}(a)$ from our $\vec{u}$ vector. It is also useful to solve Eq. (46) in the steady state and obtain

$$\rho_Q^K(d)=\frac{iG'}{\gamma_d}\sum_q[(-1)^{2F_d+q}\epsilon'_{\bar{q}}\Lambda_{cdd}^{KK'q}\rho_{Q'}^{K'}(d,c)-(-1)^{F_c+F_d+1+K'-K}(\epsilon'_{\bar{q}})^*\Lambda_{cdd}^{KK'\bar{q}}\rho_{Q'}^{K'}(c,d)]+\lambda_d^0(\gamma_d)^{-1}\delta_{K0}\delta_{Q0}\ . \tag{55}$$

If Eq. (55) is substituted into Eq. (45) and $\dot{\rho}_Q^K(c)$ is set equal to zero, one finds

$$\dot{\rho}_Q^K(c)=0=-\gamma_c\rho_Q^K(c)+\left[\frac{\gamma^K(d\to c)}{\gamma_d}\lambda_d^0+\lambda_c^0\right]\delta_{K0}\delta_{Q0}$$

$$+iG\sum_q[(-1)^{2F_c+q}\epsilon_{\bar{q}}\Lambda_{bcc}^{KK'q}\rho_{Q'}^{K'}(c,b)-(-1)^{F_b+F_c+K'-K+1}(\epsilon_{\bar{q}})^*\Lambda_{bcc}^{KK'\bar{q}}\rho_{Q'}^{K'}(b,c)]$$

$$+iG'\sum_q\{(-1)^{F_c+F_d}(\epsilon'_{\bar{q}})^*[\Lambda_{dcc}^{KK'\bar{q}}-\gamma^K(d\to c)(\gamma_d)^{-1}(-1)^{1+K'-K}\Lambda_{cdd}^{KK'\bar{q}}]\rho_{Q'}^{K'}(c,d)$$

$$-(-1)^q\epsilon'_{\bar{q}}[(-1)^{2F_c+1+K'-K}\Lambda_{dcc}^{KK'q}-\gamma^K(d\to c)(\gamma_d)^{-1}(-1)^{2F_d}\Lambda_{cdd}^{KK'q}]\rho_{Q'}^{K'}(d,c)\}\ . \tag{56}$$

Equations (44), (56), and (47)–(50) with $\dot{\rho}_Q^K=0$ are the steady-state equations which must be solved. They can be written schematically in the form

$$\underline{L}'\vec{u}+\vec{\lambda}'=\vec{0}\ , \tag{57}$$

where $\vec{u}$ is now the vector

$$\vec{u}=(\vec{\rho}(b),\vec{\rho}(b,c),\vec{\rho}(c,b),\vec{\rho}(c),\vec{\rho}(c,d),\vec{\rho}(d,c),\vec{\rho}(b,d),\vec{\rho}(d,b),\vec{\rho}(d))\ , \tag{58}$$

$\vec{\lambda}'$ is given by

$$\vec{\lambda}'=(\vec{\lambda}'(b),0,0,\vec{\lambda}'(c),0,0,0,0,\vec{\lambda}'(d));$$
$$\vec{\lambda}'(b)=\vec{\lambda}(b),$$
$$\vec{\lambda}'(c)=\vec{\lambda}(c)+[\gamma^K(d\rightarrow c)/\gamma_d]\vec{\lambda}(d), \quad (59)$$
$$\vec{\lambda}'(d)=\vec{\lambda}(d)\ ,$$

and $\underline{L}'$ is the matrix composed of the various matrix elements apearing in Eqs. (44), (56), and (47)—(50). Each element of the $\vec{u}$ and $\vec{\lambda}'$ vectors are *themselves* vectors in Liouville space (i.e., $\vec{\rho}(b)$ is composed of the $(2F_b+1)^2$ elements $\rho_Q^K(b)$ $(0\leq K\leq 2F_b,\ -K\leq Q\leq K)$, $\vec{\rho}(b,c)$ of the $(2F_b+1)(2F_c+1)$ elements $\rho_Q^K(b,c)$ $(|F_b-F_c|\leq K\leq|F_b+F_c|,\ -K\leq Q\leq K)$; $\vec{\lambda}'(b)$ of the $(2F_b+1)^2$ elements $\lambda_Q^K(b)=\lambda_b^0\delta_{K0}\delta_{Q0}$ [all but $(2F_b+1)$ of the elements are zero]; etc.) while the matrix elements $\underline{L}(f,g;r,s)$ are *themselves* matrices [i.e., $\underline{L}(b;b,c)$ is a $(2F_b+1)^2$ by $(2F_b+1)(2F_c+1)$ matrix with elements $L_{QQ'}^{KK'}(b;b,c)$; $\underline{L}(b,c;c,d)$ is a $(2F_b+1)(2F_c+1)$ by $(2F_c+1)(2F_d+1)$ matrix with elements $L_{QQ'}^{KK'}(b,c;c,d)$; etc.].

From Eqs. (44), (56), and (47)—(50), one can deduce that the matrix $\underline{L}'$ can be written in the form

$$\underline{L}'=\underline{A}+iG'\underline{B}\ , \quad (60)$$

where $\underline{A}$ has the block diagonal form shown in Table I and $\underline{B}$ the block off-diagonal form shown in Table II. (The matrix elements of $\underline{A}_1$, $\underline{A}_2$, $\underline{A}_3$ and $\underline{B}_1$, $\underline{B}_2$, $\underline{B}_3$ are listed explicitly in Appendix C.)

TABLE I. Structure of matrix $\underline{A}$. Each * indicates a nonzero matrix element.

$$\underline{A}=\begin{bmatrix}\underline{A}_1 & \underline{0} & \underline{0}\\ \underline{0} & \underline{A}_2 & \underline{0}\\ \underline{0} & \underline{0} & \underline{A}_3\end{bmatrix}$$

$\underline{A}_1=$

	b	b,c	c,b	c
b	*	*	*	*
b,c	*	*	0	*
c,b	*	0	*	*
c	0	*	*	*

$\underline{A}_2=$

	c,d	d,c	b,d	d,b
c,d	*	0	*	0
d,c	0	*	0	*
b,d	*	0	*	0
d,b	0	*	0	*

$\underline{A}_3=$

	d
d	*

TABLE II. Structure of matrix $\underline{B}$. Each * indicates a nonzero matrix element.

$$\underline{B}=\begin{bmatrix}\underline{0} & \underline{B}_1 & \underline{0}\\ \underline{B}_2 & \underline{0} & \underline{B}_3\\ \underline{0} & \underline{B}_3^\dagger & \underline{0}\end{bmatrix}$$

$\underline{B}_1=$

	c,d	d,c	b,d	d,b
b	0	0	0	0
b,c	0	0	*	0
c,b	0	0	0	*
c	*	*	0	0

$\underline{B}_2=$

	b	b,c	c,b	c
c,d	0	0	0	*
d,c	0	0	0	*
b,d	0	*	0	0
d,b	0	0	*	0

$\underline{B}_3^\dagger=$

	c,d	d,c	b,d	d,b
d	*	*	0	0

Perturbation solution for weak fields. In the limit of a weak probe field one can solve Eq. (57) in a manner that parallels the solution for the nondegenerate case.[2–13] The only difference is that elements of $\vec{u}$ are now vectors (instead of scalars) and matrix elements of the $\underline{A}$ and $\underline{B}$ matrices which comprise $\underline{L}'$ are now matrices instead of scalars.

As in the nondegenerate case, one assumes a solution

$$\vec{u}=\sum_n \vec{u}^{(n)},\quad \vec{u}^{(n)}\propto(G')^n \quad (61)$$

and equates various orders of G' in Eq. (57). In this paper, we calculate the upper-state density-matrix elements $\rho_Q^K(d)$ to second order in G'. Therefore we set

$$\vec{u}=\vec{u}^{(0)}+\vec{u}^{(1)}+\vec{u}^{(2)} \quad (62)$$

and using Eqs. (60) and (61), find

$$\vec{u}^{(0)}=-\underline{A}^{-1}\vec{\lambda}'\ , \quad (63)$$
$$\vec{u}^{(1)}=-iG'\underline{A}^{-1}\underline{B}\vec{u}^{(0)}\ , \quad (64)$$
$$\vec{u}^{(2)}=-iG'\underline{A}^{-1}\underline{B}\vec{u}^{(1)}\ . \quad (65)$$

Given the structure of the $\underline{L}'$ matrix, it is convenient to separate the $\vec{u}$ vector as

$$\vec{u}=(\vec{u}_1,\vec{u}_2,\vec{u}_3)\ , \quad (66)$$

where $\vec{u}_1$, $\vec{u}_2$, and $\vec{u}_3$ are the vectors

$$\vec{u}_1=(\vec{\rho}(b),\vec{\rho}(b,c),\vec{\rho}(c,b),\vec{\rho}(c)) ,$$
$$\vec{u}_2=(\vec{\rho}(c,d),\vec{\rho}(d,c),\vec{\rho}(b,d),\vec{\rho}(d,b)) , \quad (67)$$
$$\vec{u}_3=\vec{\rho}(d) .$$

It is now fairly straightforward to carry out the calculations in Eqs. (63)—(65). Taking into account the form of $\vec{\lambda}'$ and $\underline{A}$ we first calculate

$$\vec{u}^{(0)}=-\underline{A}^{-1}\vec{\lambda}'=(\vec{u}_1^{(0)},\vec{0},\vec{u}_3^{(0)}) , \quad (68)$$

where

$$\begin{aligned}
&\vec{\rho}^{(0)}(b)=\vec{u}_1^{(0)}(b)=-[\underline{A}_1^{-1}(b;b)\vec{\lambda}'(b)+\underline{A}_1^{-1}(b;c)\vec{\lambda}'(c)],\\
&\vec{\rho}^{(0)}(b,c)=\vec{u}_1^{(0)}(b,c)=-[\underline{A}_1^{-1}(b,c;b)\vec{\lambda}'(b)+\underline{A}_1^{-1}(b,c;c)\vec{\lambda}'(c)] ,\\
&\vec{\rho}^{(0)}(c,b)=\vec{u}_1^{(0)}(c,b)=-[\underline{A}_1^{-1}(c,b;b)\vec{\lambda}'(b)+\underline{A}_1^{-1}(c,b;c)\vec{\lambda}'(c)] ,\\
&\vec{\rho}^{(0)}(c)=\vec{u}_1^{(0)}(c)=-[\underline{A}_1^{-1}(c;b)\vec{\lambda}'(b)+\underline{A}_1^{-1}(c;c)\vec{\lambda}'(c)] ,\\
&\vec{\rho}^{(0)}(d)=\vec{u}_3^{(0)}(d)=-\underline{A}_3^{-1}\vec{\lambda}'(d)=\vec{\lambda}'(d)/\gamma_d .
\end{aligned} \quad (69)$$

Formal expressions can be written for the inverse matrices which appear in Eq. (69); these terms include the saturation effects of the strong field. Rather than list these expressions (which are somewhat unwieldly), we shall simply assume that computer solutions have given us values of $\vec{u}^{(0)}$ as a function of pump-field amplitude G and atom—pump-field detuning Δ.

Having obtained $\vec{u}^{(0)}$, we form the product

$$\vec{c}=(\vec{c}_1,\vec{c}_2,\vec{c}_3)=\underline{B}\vec{u}^{(0)} \quad (70)$$

and find

$$\vec{c}_1=\vec{0}, \quad \vec{c}_2=\underline{B}_2\vec{u}_1^{(0)}+\underline{B}_3\vec{u}_3^{(0)}, \quad \vec{c}_3=\vec{0} . \quad (71)$$

Using this result and Eq. (64), we obtain

$$\vec{u}^{(1)}=-iG'\underline{A}^{-1}\vec{c}=(\vec{u}_1^{(1)},\vec{u}_2^{(1)},\vec{u}_3^{(1)}) , \quad (72)$$

where

$$\vec{u}_1^{(1)}=\vec{0}, \quad \vec{u}_2^{(1)}=-iG'\underline{A}_2^{-1}\vec{c}_2, \quad \vec{u}_3^{(1)}=\vec{0} . \quad (73)$$

Finally, the second-order contribution to $\vec{u}$ is given by

$$\vec{u}^{(2)}=-iG'\underline{A}^{-1}\underline{B}\vec{u}^{(1)}=(\vec{u}_1^{(2)},\vec{u}_2^{(2)},\vec{u}_3^{(2)}) , \quad (74)$$

where

$$\begin{aligned}
&\vec{u}_1^{(2)}=-iG'\underline{A}_1^{-1}\underline{B}_1\vec{u}_2^{(1)} ,\\
&\vec{u}_2^{(2)}=\vec{0} ,\\
&\vec{u}_3^{(2)}=-iG'\underline{A}_3^{-1}\underline{B}_3^{\dagger}\vec{u}_2^{(1)} .
\end{aligned} \quad (75)$$

Therefore, to second order in the probe field, the upper-state density-matrix elements are given by

$$\begin{aligned}
\vec{\rho}(d)&=\vec{u}_3^{(0)}+\vec{u}_3^{(2)}\\
&=\frac{\vec{\lambda}'(d)}{\gamma_d}+\frac{(G')^2}{\gamma_d}\underline{B}_3^{\dagger}\underline{A}_2^{-1}(\underline{B}_2\vec{u}_1^{(0)}+\underline{B}_3\vec{u}_3^{(0)}) .
\end{aligned} \quad (76)$$

The matrix $(\underline{A}_2)^{-1}$ may be easily calculated and the matrix operations implicit in Eq. (76) can be carried out to obtain

$$\begin{aligned}
\vec{\rho}(d)=\vec{\lambda}'(d)/\gamma_d&-[(G')^2/\gamma_d](\underline{B}_3^{\dagger}(d;c,d)[\eta_{bc}\eta_{cd}+\underline{A}_2(c,d;b,d)\underline{A}_2^{\dagger}(c,d;b,d)]^{-1}\\
&\times\{\eta_{bd}[\underline{B}_2(c,d;c)\vec{\rho}^{(0)}(c)+\underline{B}_3(c,d;d)\vec{\rho}^{(0)}(d)]+\underline{A}_2(c,d;b,d)\underline{B}_2(b,d;b,c)\vec{\rho}^{(0)}(b,c)\}\\
&+\underline{B}_3^{\dagger}(d;d,c)[\eta_{bd}^{*}\eta_{cd}^{*}+\underline{A}_2(d,c;c)\underline{A}_2^{\dagger}(d,c;c)]^{-1}\\
&\times\{\eta_{bd}^{*}[\underline{B}_2(d,c;c)\vec{\rho}^{(0)}(c)+\underline{B}_3(d,c;d)\vec{\rho}^{(0)}(d)]+\underline{A}_2(d,c;d,b)\underline{B}_2(d,b;c,b)\vec{\rho}^{(0)}(c,b)\}) ,
\end{aligned} \quad (77)$$

where

$$\begin{aligned}
&\eta_{cd}=\gamma_{cd}+i\Delta' ,\\
&\eta_{bd}=\gamma_{bd}+i(\Delta+\Delta') .
\end{aligned} \quad (78)$$

In this form, the expression for $\vec{\rho}(d)$ is closely related to the analogous expression obtained in the nondegenerate case.[2—13]

The method of calculation is as follows: For a given value of G and Δ, the matrix $\underline{A}_1$ is inverted so that values of $\vec{\rho}^{(0)}$ may be obtained; then, the upper-state density-matrix elements $\rho_Q^K(d)$ are found by performing the necessary matrix manipulations of Eq. (77). Results are presented in Sec. VI.

VI. APPLICATION OF THE FORMALISM

The formalism developed in the previous sections can be used to derive theoretical expressions for probe absorption line shapes which can then be compared with experimental profiles. For laser fields interacting with an atomic vapor confined to a cell, it is necessary to average Eq.

(77) over the atomic velocity distribution. In this work, we consider the somewhat simpler situation of laser fields interacting with an atomic beam, for which no velocity-averaging is needed. For the atomic-beam—laser-field interaction, we explore the effects of optical pumping and saturation in systems of three degenerate atomic energy states, doubly excited by an arbitrarily strong pump field and a weak probe field, using different arrangements of the polarizations of the two fields.

We will thus use the formalism to describe the behavior of a beam of atoms entering and passing through an arrangement of two laser fields, so that the atomic beam and the two laser fields are mutually perpendicular to each other. The atoms are in their ground state when they enter the interaction region and we wish to calculate the average distribution of upper-state population for atoms at all stages of transit through the laser fields. This might be monitored experimentally, for example, by observing fluorescence from the uppermost level. We may model this essentially dynamical system by finding the steady-state solution of Eq. (57), when $\vec{\lambda}'$ contains the rates of creation or entry of ground-state atoms into the beam, and the diagonal elements of $\underline{\underline{L}}'$ include a damping term representing the loss of atoms are they pass out of the path of the laser fields. A subtle assumption is implied by solving Eq. (57) in this manner, which is that atoms have an equal probability of disappearing from the beam at any point along the path of transit through the laser fields, rather than just at one point of exit. This is clearly unphysical, but it may be easily shown that for $\gamma_c/\Gamma_e > 10$, where γ_c is the rate of spontaneous decay of level c (see Fig. 3) and Γ_e the rate of exit of atoms from the beam, the solution of the steady-state problem with a homogeneous decay rate Γ_e is approximately equal to that of the time-dependent problem of interest. In this limit, the solutions obtained by this method will demonstrate the characteristics of saturation and optical pumping in the systems we are modeling, and provide useful insights in a more concise and less time-consuming way than by the time-dependent calculations that would otherwise be required.

We will assume that the atoms effectively enter the two fields simultaneously; and that any variation of Γ_e with velocity can be neglected, so that no velocity-averaging over the final spectrum is necessary. We will also assume that the field strength of the two lasers is constant over the cross-sectional area of illumination, and that relaxation between the atomic states takes place by spontaneous emission only.

We have chosen to apply the formalism to a manifold of three degenerate atomic hyperfine states b,c,d, with total angular momentum quantum numbers $F_b=1$, $F_c=2$, and $F_d=3$, in order of increasing energy, respectively. For our primary purposes here, we will not consider a lower state a (see Fig. 3) into which the atom can be pumped by spontaneous emission from state c, but will concern ourselves with the pumping processes within the manifold b,c,d only. However, we will provide a brief discussion of the effect of a fourth level, a, at a later stage.

We are then seeking to describe how the population of the atomic state d changes as the atoms enter and pass through the region of illumination of the two laser fields. We calculate the steady-state population $N(d)$ as a function of probe detuning Δ' for various values of (1) pump-field strength G, (2) relaxation parameters γ_c, $\gamma(c\rightarrow b)$, and $\gamma(c\rightarrow a)$, (3) pump-field detuning Δ, and (4) pump- and probe-field polarizations. For a given pump-field detuning Δ, pump-field strength parameter G, and pump-field polarization, a computer solution of Eq. (68) provides values for $\vec{\rho}^{(0)}(c)$, $\vec{\rho}^{(0)}(d)$, $\vec{\rho}^{(0)}(b,c)$, and $\vec{\rho}^{(0)}(c,b)$. These quantities are then substitutied into Eq. (77) from which one calculates the final-state density-matrix $\vec{\rho}(d)$ as a function of probe-field detuning and polarization. [The A and B matrices needed in Eqs. (68) and (77) are given in Appendix C.] In all the calculations, the atoms are assumed to enter the interaction region in an unpolarized ground state. All frequencies are given in units of the inverse transit time Γ_e.

In order to calculate the transition matrix elements for the three-level manifold of states introduced above, we have considered them to be part of a set of electron fine-structure states of Na. Thus the three-level system may be more completely labeled $3S_{1/2}$ $(F=1)\leftrightarrow 3P_{1/2}$ $(F=2)\leftrightarrow 4D_{3/2}$ $(F=3)$. The series of curves in Figs. 4(a)—4(e) show the distribution of population $N(d)=\sqrt{7}\rho_0^0(d)$ in the uppermost level d [$4D$ $(F=3)$], for a *circularly* polarized pump field held on resonance $(\Delta=0)$ as a function of the probe-field detuning Δ' for several values of G. We have taken (in units of Γ_e) $\lambda_d^0=\lambda_c^0=0$; $\lambda_b^0=\sqrt{3}$ (corresponding to unit population in state b in the absence of all fields), $\gamma_b=0$, and $\gamma_c=\gamma(c\rightarrow b)=\gamma_d=50$. The probe field is linearly polarized and its strength parameter G' is chosen such that perturbation theory is valid. In particular, a value $G'^2/\gamma_c\gamma_{cd}\simeq 3.889\times 10^{-3}\ll 1$ was assumed leading to values for the upper-state populations shown in Figs. 4(a)—4(e). This value for G' corresponds to a laser power density of order 1.0 W/m^2; the upper-state population varies as G'^2 in the perturbation limit. It may be seen in Fig. 4(a) that with a value of pump-field strength less than the relaxation rates, the population in the uppermost level has a single-peaked, Lorentzianlike distribution. However, as the pump field is increased, we see that this structure first separates into two peaks [Fig. 4(c)] due to the Rabi splitting, and later [Figs. 4(d) and 4(e)] separates into six clearly distinguishable peaks This effect is explained by the fact that the magnitude of the Rabi splitting of the upper resonance depends linearly upon the product of the pump-laser-field amplitude and the matrix element for the pump transition. Since the lower pair of levels $(F=1$, $F=2)$ are irradiated by circularly polarized light the pump laser effectively drives three transitions, with distinct matrix elements, between them. For example, if the selection rule $\Delta M=+1$ applies, then the field will drive the following three transitions: $(F=1,\ M=-1)\rightarrow(F=2,\ M=0)$; $(F=1,\ M=0)\rightarrow(F=2,\ M=1)$; $(F=1,\ M=1)\rightarrow(F=2,\ M=2)$. Calculation quickly shows that it is the last of these three which has the largest transition matrix element. Therefore, as the pump field is increased, the presence of three transitions leads to

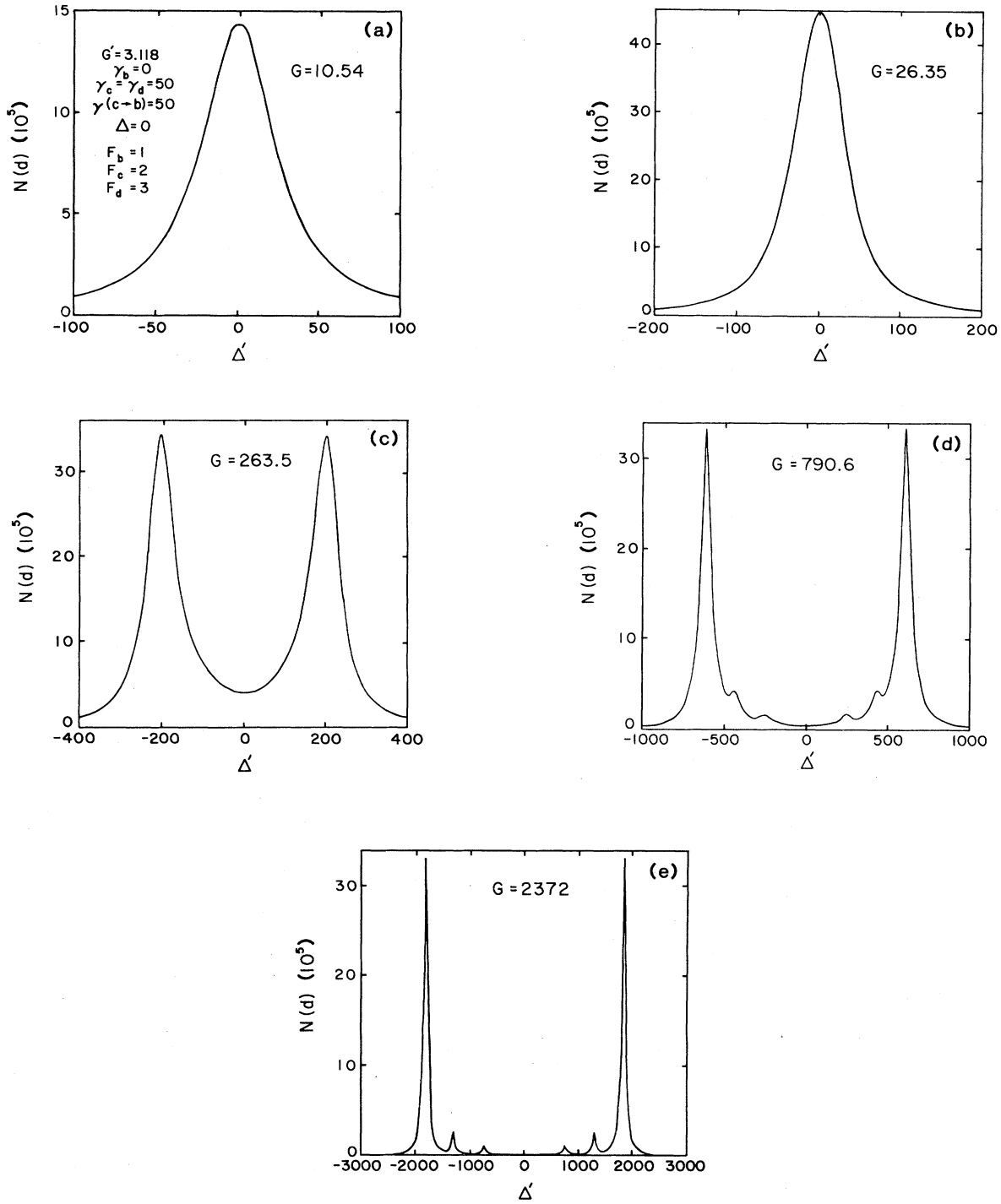

FIG. 4. Probe absorption line shape [upper-state population $N(d)$ as a function of probe detuning Δ'] for a circularly polarized pump field and a linearly polarized probe field as a function of the pump-field amplitude factor G. (a)—(e) give results for $G=10.54$, 26.35, 263.5, 790.6, and 2372, respectively. Values of F_b, F_c, and F_d are 1, 2, and 3. All frequencies are in units of Γ_e (Γ_e^{-1} is effectively the atom's transit time through the laser fields).

the appearance of six Rabi lobes: three sets of two, symmetrically displaced on either side of the position of the original, unsplit resonance. The pump transition with the largest matrix element $(F=1, M=\pm 1) \rightarrow (F=2, M=\pm 2)$ will give rise to the most widely displaced pair of lobes in the probe, the others being displaced to a smaller degree proportional to the other matrix elements in the pump transition.

Apart from differences in the Clebsch-Gordan coefficients associated with the upper-state transitions, the ex-

planation of the differences in the intensities of the Rabi lobes in Figs. 4(d) and 4(e), as opposed to their position, depends upon the effects of optical pumping between the lower level b ($F=1$) and the center level c ($F=2$). As we have seen, the circularly polarized pump field induces transitions with $\Delta M=\pm 1$ between b and c. However, when the atom is in state c, spontaneous emission may lead to its decay back down to b, and since the tensor quantities $\rho_Q^K(c)$ decay diagonally "into" their counterparts $\rho_Q^K(b)$ [see Eqs. (35) and (36)], indicating that relaxation processes will occur with selection rules $\Delta M=0,\pm 1$. The net effect will be a transfer of population, by stepwise optical pumping, along the series of degenerate levels (if say $\Delta M=+1$ for the radiative process) towards the $F=2$, $M=+2$ level. We have seen that pumping on the ($F=1$, $M=1$)$\rightarrow$($F=2$, $M=2$) transition leads to the most widely displaced Rabi lobes and since there is a tendency for population buildup in the ($F=2$, $M=2$) level by optical pumping, this will lead to increased population transfer to the uppermost level d at these lobe frequencies, i.e., the intensity of the outer Rabi lobes is enhanced with respect to the others by the optical-pumping effect. Certain properties of the saturation of level c may be seen in Figs. 4(c)—4(e). Note that the intensity of the split lobes does not increase with increasing field strength. The population of level c is already saturated by the pump field in Fig. 4(c); further increases in G serve only to increase the Rabi splitting. It is also interesting to note that the peak intensity in Fig. 4(b) is greater than that in Fig. 4(e). At the pump-field strength of Fig. 4(b), saturation of level c is not complete, but interference effects between "stepwise" and "two-quantum" excitation processes lead to a larger intensity.

The intensity ratio of the lobes depends upon the pump-field strength, the rates of spontaneous relaxation and the upper-state Clebsch-Gordan coefficients. The effect of a reduced spontaneous-decay rate is clearly seen in Fig. 5, which is drawn with $\gamma_c=10$, but other parameters the same as in Fig. 4(e). The difference in intensity of the various Rabi lobes is not as marked as in Fig. 4(e). This feature can be explained by noting that, in the strong saturation limit, the ratio of population in the $M=2$ sublevel of state c (which drives the outer lobes), to the total population in that state, varies from $\frac{1}{3}$ to 1 as γ_c/Γ_e varies from a value much less than unity to a value much greater than unity.

In Fig. 6, we show the spectrum of population distribution in level d when optical pumping does not occur. This (artificial) condition of no optical pumping is simulated by neglecting the spontaneous emission from level c into level b and considering level c to decay entirely into level a [see Fig. 3). In the calculations, all other parameters are unchanged from those used to obtain the curve shown in Fig. 4(e). In Fig. 6, we see that the position of the Rabi lobes remains unchanged. However, since no optical pumping has occurred, the outermost lobes are no longer the most intense. At this level of the pump field, all of the active degenerate levels in c are saturated to the same population, and it may easily be shown that the intensities of the Rabi lobes now vary in proportion to the transition strengths between these levels and those in d ($F=3$) to which they are connected by the linearly polarized probe field. The fact that the peak intensities are lower than those shown in Fig. 4(e) is due to the loss of population to level a.

The case of a nonzero pump-field detuning, and no optical pumping, is shown in Fig. 7. As in the $\Delta=0$ case (see Fig. 6), six resonances may be seen, but the symmetric nature of the solution is lost. The precise positions of the resonances in this strong-field case may be calculated using the equations in Appendix A.

In Fig. 8 is displayed the distribution of population in level d when both pump and probe transitions are irradiated with radiation having the same direction of linear polarization. It is seen that in this case only two Rabi lobes appear on either side of the original resonance for large values of the pump field. This is a consequence of the fact that when linearly polarized radiation is applied, the pump transition ($F=1\rightarrow F=2$) has three components ($M=0,\pm 1$) as in the circularly polarized case, but now two of them ($M=\pm 1$) have identical transition strengths and so induce the same amount of Rabi splitting on the probe transition. In this case, the effects of spontaneous

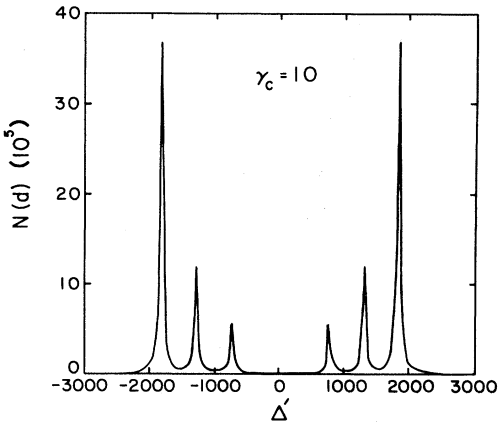

FIG. 5. Effect of a reduced decay rate for level c. All other parameters as in Fig. 4(e).

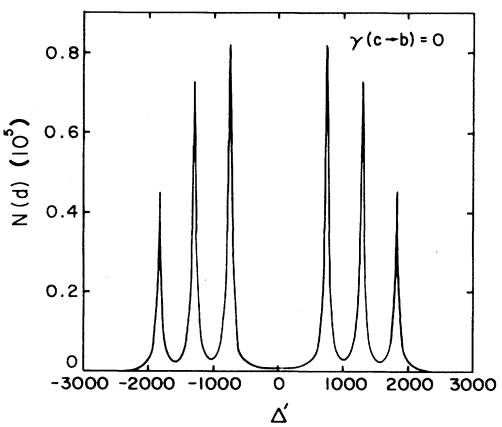

FIG. 6. Artificial suppression of optical-pumping effects by taking $\gamma(c\rightarrow b)=0$. All other parameters as in Fig. 4(e).

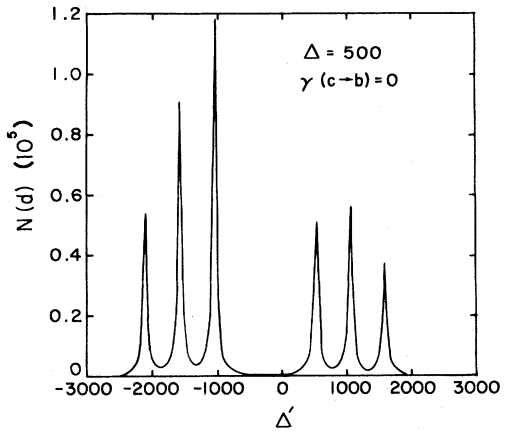

FIG. 7. Effect of a nonzero detuning $\Delta=500$, with no optical pumping. All other parameters as in Fig. 6.

emission out of c into b do not lead to an anomalously large value for one of the transitions relative to the others, since optical pumping produces only a slight buildup of population in the $M=0$ substate of level c. In the saturation limit, the ratio of the population of the $M=0$ sublevel of state c (which drives the outer lobes) to the total population in that state, varies from $\frac{1}{3}$ to 0.6 as γ_c/Γ_e varies from a value much less than unity to a value much greater than unity.

The case of an elliptically polarized pump field and a *copropagating* linearly polarized probe field is illustrated in Figs. 9(a)–9(e) for a $F_b=1$, $F_c=F_d=2$ three-level system with no optical pumping. The probe field is polarized in the x direction and the pump field's polarization is specified by the angle

$$\alpha=\tan^{-1}\left|\frac{\epsilon_y}{\epsilon_x}\right| . \tag{79}$$

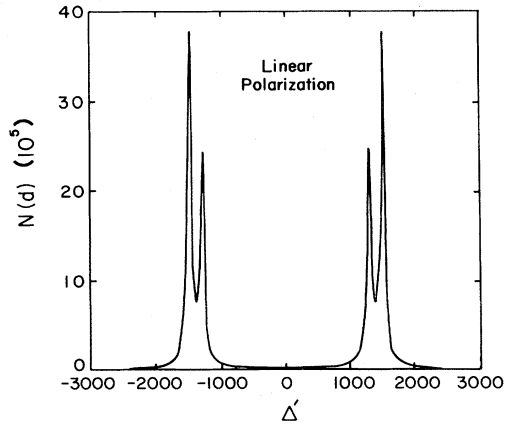

FIG. 8. Effect of a linearly polarized pump field, including effects of optical pumping. All other parameters as in Fig. 4(e).

All graphs are drawn in the strong-field limit. For $\alpha=0°$ (collinearly polarized), two peaks are seen (four peaks would normally be seen, but selection rules for the upper transition suppress one pair of resonances). For elliptic ($\alpha=22.5°$ or $67.5°$) polarization, or circular polarization ($\alpha=45°$), six resonance peaks are seen. The positions of two of these peaks are fixed, while the positions of four of them vary with the pump polarization, all other parameters held constant. Finally, for cross-polarized fields ($\alpha=90°$), two of the peaks coalesce into the fixed peaks so that a total of four distinct peaks occur. A method for predicting the positions of the resonances is given in Appendix B using a dressed-atom approach to the problem. Note that the resonance *positions* in Figs. 9(a) and 9(c) are identical with those in Figs. 8 and 4(e), respectively, since it is the *pump*-field amplitude and polarization which determines these positions. Since level c is saturated by the pump field, the relative peak heights of the resonances are determined by the Clebsch-Gordan coefficients associated with the c-d transition.

Returning to the case of a circularly polarized pump, and with the same field strengths and relaxation rates used in Figs. 4(e) and 6, we show in Fig. 10 the spectrum of population in the upper level d when we include a second ground-state level a to which atoms in state c may decay by spontaneous emission, as shown in Fig. 3. This situation differs from that of Fig. 6 in that level c decays into both levels b and a rather than into level a alone. Bearing in mind the Na manifold mentioned above, we have used the $3S_{1/2}$ ($F=2$) hyperfine level as the second ground state in this case. After atoms are excited from $3S_{1/2}$ ($F=1$)$\rightarrow 3P_{1/2}$ ($F=2$), they may decay spontaneously to either $3S_{1/2}$ ($F=1$) or $3S_{1/2}$ ($F=2$) as determined by the branching ratio given by standard theory. Examination of Fig. 10 shows that the positions of the Rabi lobes are identical to those in the circularly polarized cases represented by Figs. 4(e), 5, and 6, where the pump-field strength is the same. However, the intensity ratio of the lobes is different from that of either Fig. 4(e) or Fig. 6, although the total rate of spontaneous relaxation from level c is the same. Some elements of the stepwise optical-pumping effect, leading to buildup of population in the $M=+2$ level of the $3P_{1/2}$ ($F=2$) state, are still apparent. The most widely displaced Rabi lobe is still the most intense, but the effect is much reduced. The optical pumping of state c has been reduced owing to the fact that the system is no longer "closed"; population from the $M=-1$ and $M=0$ substates of level b no longer transfer all of their population to the $M=1$ substate, since some population is lost to level a along the way. The overall population of level b (and, consequently, that of level d) is greatly reduced owing to the fact that a population of order $\gamma_c/(\gamma_c+\Gamma_e)\simeq 1$ is transferred to level a (leaving a steady-state population of order $\Gamma_e/\gamma_c \ll 1$ in level b) by the combined processes of laser pumping and spontaneous emission. The ratio of the Rabi lobe intensities is intermediate between that shown in Figs. 4(e) and 6. It may be noted that level a can become polarized as a result of the optical-pumping process. Under certain experimental conditions, it may prove convenient to monitor this polarization.

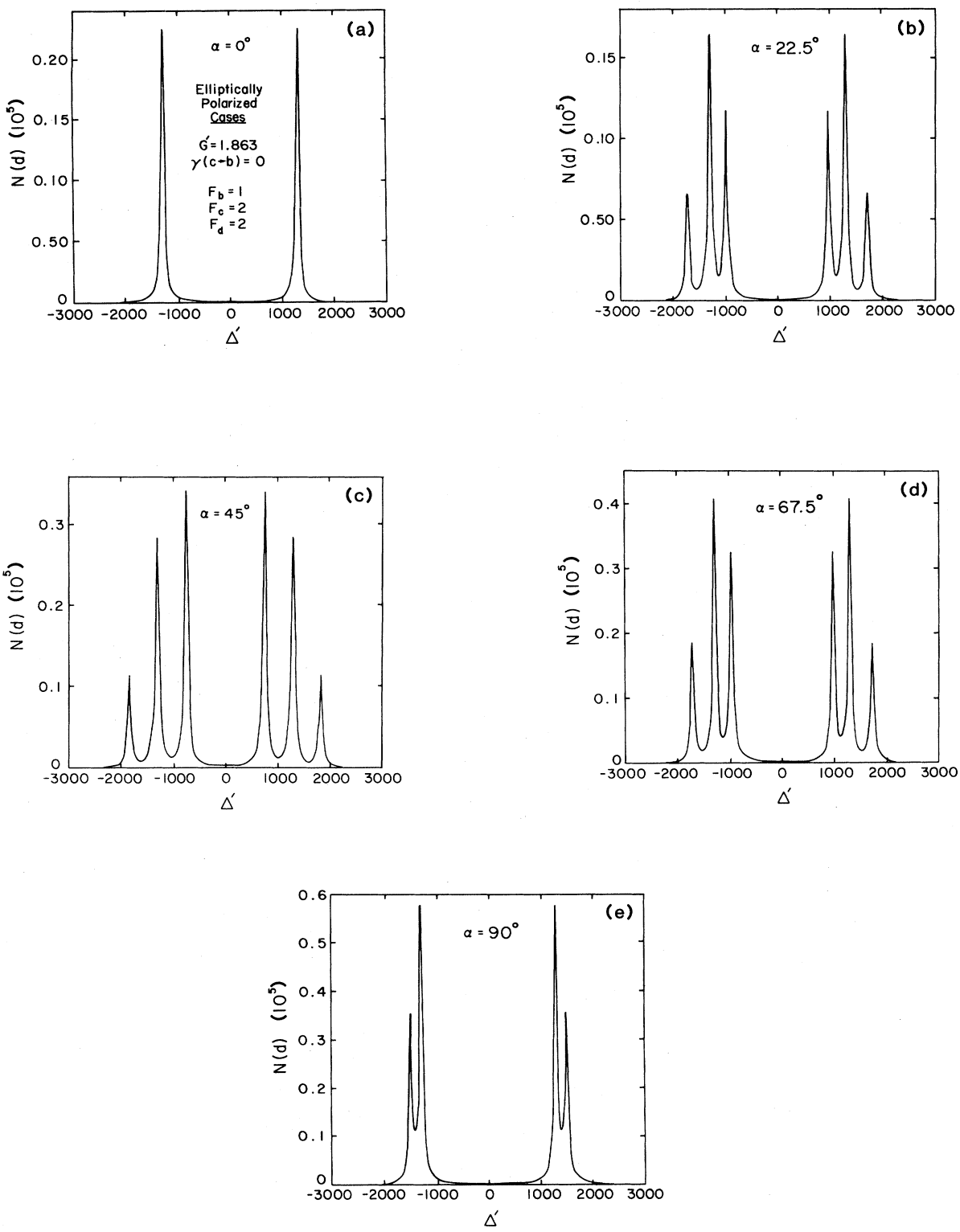

FIG. 9. Effect of an elliptically polarized pump field: $\alpha=0°$, collinear polarization; $\alpha=45°$, circular polarization; $\alpha=90°$, cross polarized. Values of F_b, F_c, and F_d are 1, 2, and 2 and there is no optical pumping. All other parameters as in Fig. 6.

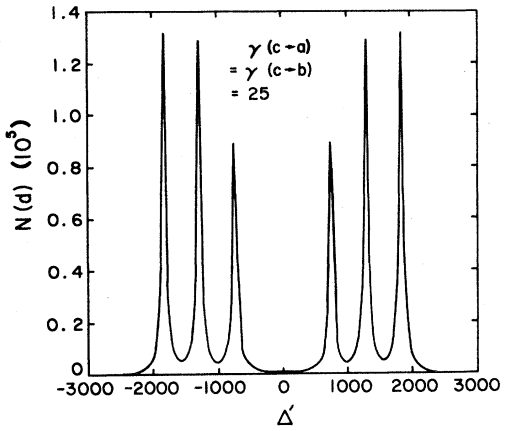

FIG. 10. Modification of optical pumping when level c has two decay channels. All other parameters as in Fig. 4(e).

VII. CONCLUSION

By using the methods of saturation and coherent transient spectroscopy for three-level systems, one is able to obtain Doppler-free line shapes from which values for various parameters of physical interest may be extracted. In this paper, we have developed a theory which can be applied to problems in which a pump laser field drives a transition between levels "1" and "2" while a probe laser field drives a coupled transition between levels "2" and "3." Each "level" (1, 2, or 3) was assumed to consist of a number of degenerate or nearly degenerate substates so that the theory could be applied to "real" systems.

Although the present calculation was somewhat restricted (laser fields of constant amplitudes, a single velocity subclass of atoms, a "weak" probe field, no collisional relaxation), the formalism is applicable to a wide range of problems involving steady-state or transient laser fields. Moreover, the theory can be extended to include collisional effects, enabling one to analyze experimental results such as those obtained recently[61] in an experiment in which optical pumping and collisions modify the line shapes observed in the $3S\rightarrow 3P\rightarrow 4D$ excitation of sodium.

A density-matrix (rather than amplitude) formulation must be used to incorporate relaxation processes (such as optical pumping) into the calculation. The irreducible tensor representation adopted in the text will prove particularly useful when the relaxation phenomena (spontaneous emission, collisions) possess some type of spherical symmetry; in that case, the equations governing the relaxation take on a particularly simple form in the irreducible tensor basis. However, as noted in Appendix A, there may be cases in which the standard (m-basis) representation offers some advantages over the irreducible tensor one.

Finally, it should be noted that our approach differs from that recently proposed by Morris and Shore.[62] Their calculation of state amplitudes in two-level degenerate systems involves a choice of bases which reduces the problem to an analytically soluble form; their method is applicable to fields of constant polarization (but whose amplitudes may vary with time) interacting with atomic systems in which relaxation processes can be neglected.

ACKNOWLEDGMENTS

It is a pleasure to acknowledge several helpful discussions with Professor E. Robinson of New York University. This research is supported by the U. S. Navy Office of Naval Research.

APPENDIX A: SOLUTION IN THE STANDARD REPRESENTATION

The irreducible tensor notation is particularly useful in problems involving relaxation, since symmetry considerations reduce the number of relaxation parameters which enter to a minimum. However, if there is *no* collisional coupling between magnetic substates, it may prove advantageous to use the standard representation rather than the irreducible tensor one. For example, consider a transition $J_1\rightarrow J_2$ $(J_2>J_1)$ induced by linearly polarized radiation, in which optical pumping is not present. In the standard representation, this problem reduces to a set of $(2J_1+1)$ individual two-level problems between states (J_1,m) and (J_2,m). On the other hand, no such reduction into two-level subspaces is possible in the irreducible tensor notation, owing to the linear combination of magnetic substates which appears.

The standard representation is particularly useful when (1) radiation fields coupling the various levels are either circularly or linearly polarized and (2) no collisional relaxation is present. In this appendix, we use the standard representation to obtain a steady-state solution to the three-level problem subject to the above restrictions. It should be noted that this appendix is essentially self-contained.

The three-level system under consideration consists of levels b, c, and d, having total angular momenta F_b, F_c, and F_d, respectively. Each level actually consists of $(2F+1)$ degenerate magnetic substates. As viewed in the atomic rest frame, levels b and c are coupled by the radiation field

$$\vec{\mathrm{E}}(t)=\tfrac{1}{2}(\vec{\mathscr{E}}e^{i\Omega t}+\vec{\mathscr{E}}^{*}e^{-i\Omega t}) \tag{A1a}$$

and levels c and d by the field

$$\vec{\mathrm{E}}'(t)=\tfrac{1}{2}(\vec{\mathscr{E}}'e^{i\Omega' t}+\vec{\mathscr{E}}'^{*}e^{-i\Omega' t}) , \tag{A1b}$$

where the Doppler-shifted frequencies Ω and Ω' are related to the radiation field frequencies Ω_L and Ω'_L by

$$\Omega=\Omega_L-\vec{\mathrm{k}}\cdot\vec{\mathrm{v}} , \quad \Omega'=\Omega'_L-\vec{\mathrm{k}}'\cdot\vec{\mathrm{v}} . \tag{A2}$$

The propagation constants k and k' are defined by $k=\Omega_L/c$ and $k'=\Omega'_L/c$, and $\vec{\mathrm{v}}$ is the atomic velocity. The (complex) field amplitudes are written in the form

$$\vec{\mathscr{E}}=\hat{\epsilon}\,|\,\vec{\mathscr{E}}\,| , \quad \vec{\mathscr{E}}'=\hat{\epsilon}'\,|\,\vec{\mathscr{E}}'\,| , \tag{A3}$$

where $\hat{\epsilon}$ and $\hat{\epsilon}'$ are now complex unit vectors subject to the restrictions

$$\vec{\mathrm{k}}\cdot\hat{\epsilon}=0 , \quad \vec{\mathrm{k}}'\cdot\hat{\epsilon}'=0 . \tag{A4}$$

It is still convenient to express the interaction potential $U=-\vec{D}\cdot(\vec{E}+\vec{E}')$ in terms of components of irreducible tensor operators of rank 1 as

$$U(t)=-\tfrac{1}{2}[(-1)^q D_q \mid \vec{\mathscr{E}} \mid e^{i\Omega t} + (-1)^{q'} D_{q'} \mid \vec{\mathscr{E}}' \mid e^{i\Omega' t}] + \text{H.c.} , \tag{A5}$$

where q can be equal to -1, 0, or 1, q' can be equal to -1, 0, or 1, and the irreducible components of $\vec{D}$ are defined by

$$D_{\pm 1}=\mp\frac{1}{\sqrt{2}}(D_x+iD_y) , \tag{A6}$$

$$D_0=D_z .$$

The fact that q and q' each are restricted to a single value implies that the radiation fields are either linearly or circularly polarized.[63] In the form (A5), it is an easy matter to calculate the necessary matrix elements appearing in the Schrödinger equation.

In terms of a field interaction representation to be defined below, the equations of motion for the density-matrix elements (in the rotating-wave approximation) are

$$\frac{\partial\rho_{mm'}(b)}{\partial t}=-\gamma_b\rho_{mm'}(b)+\lambda_m(b)\delta_{mm'}+\sum_{p,p'}\gamma^{pp'}_{mm'}(c\to b)\rho_{pp'}(c)+iG_{m,m+q}\tilde{\rho}_{m+q,m'}(c,b)-iG_{m',m'+q}\tilde{\rho}_{m,m'+q}(b,c) , \tag{A7a}$$

$$\frac{\partial\rho_{mm'}(c)}{\partial t}=-\gamma_c\rho_{mm'}(c)+\lambda_m(c)\delta_{mm'}+\sum_{\alpha=b,d}\sum_{p,p'}\gamma^{pp'}_{mm'}(\alpha\to c)\rho_{pp'}(\alpha)+iG_{m-q,m}\tilde{\rho}_{m-q,m'}(b,c) - iG_{m'-q,m}\tilde{\rho}_{m,m'-q}(c,b)+iG'_{m,m+q}\tilde{\rho}_{m+q',m'}(d,c)-iG'_{m',m'+q'}\tilde{\rho}_{m,m'+q'}(c,d) , \tag{A7b}$$

$$\frac{\partial\rho_{mm'}(d)}{\partial t}=-\gamma_d\rho_{mm'}(d)+\lambda_m(d)\delta_{mm'}+\sum_{p,p'}\gamma^{pp'}_{mm'}(c\to d)\rho_{pp'}(c)+iG'_{m-q',m}\tilde{\rho}_{m-q',m'}(c,d)-iG'_{m'-q',m'}\tilde{\rho}_{m,m'-q'}(d,c) , \tag{A7c}$$

$$\frac{\partial\tilde{\rho}_{mm'}(b,c)}{\partial t}=-\eta_{bc}\tilde{\rho}_{mm'}(b,c)+iG_{m,m+q}\rho_{m+q,m'}(c)-iG_{m'-q,m'}\rho_{m,m'-q}(b)-iG'_{m',m'+q'}\tilde{\rho}_{m,m'+q'}(b,d) , \tag{A7d}$$

$$\frac{\partial\tilde{\rho}_{mm'}(c,d)}{\partial t}=-\eta_{cd}\tilde{\rho}_{mm'}(c,d)+iG'_{m,m+q'}\rho_{m+q',m'}(d)-iG'_{m'-q',m'}\rho_{m,m'-q'}(c)+iG_{m-q,m}\tilde{\rho}_{m-q,m'}(b,d) , \tag{A7e}$$

$$\frac{\partial\tilde{\rho}_{mm'}(b,d)}{\partial t}=-\eta_{bd}\tilde{\rho}_{mm'}(b,d)+iG_{m,m+q}\tilde{\rho}_{m+q,m'}(c,d)-iG'_{m'-q',m'}\tilde{\rho}_{m,m'-q'}(b,c) , \tag{A7f}$$

$$\tilde{\rho}_{mm'}(\alpha,\beta)=[\tilde{\rho}_{m'm}(\beta,\alpha)]^* . \tag{A7g}$$

The various terms appearing in these equations are as follows. (1) The variables $\tilde{\rho}$ are defined by the field-interaction representation,

$$\rho(b,c)=\tilde{\rho}(b,c)e^{i\beta\Omega t} , \tag{A8a}$$

$$\rho(c,d)=\tilde{\rho}(c,d)e^{i\beta'\Omega' t} , \tag{A8b}$$

$$\rho(b,d)=\tilde{\rho}(b,d)e^{i(\beta\Omega+\beta'\Omega')t} . \tag{A8c}$$

The quantities β and β' can take on the values of ± 1 to indicate the type of three-level system under consideration. For the upward cascade ($\omega_{cb}>0$, $\omega_{dc}>0$), $\beta=\beta'=1$; for the V configuration ($\omega_{cb}<0$, $\omega_{dc}>0$), $\beta=-1$, $\beta'=1$; for the Λ configuration ($\omega_{cb}>0$, $\omega_{dc}<0$), $\beta=1$, $\beta'=-1$.[64] (2) The quantity γ_α ($\alpha=b,c,d$) is the decay rate out of state α. (3) The quantity $\gamma^{pp'}_{mm'}(\alpha\to\alpha')$ is the rate at which spontaneous emission creates $\rho_{mm'}(\alpha')$ from $\rho_{pp'}(\alpha)$. Explicitly, one finds

$$\gamma^{pp'}_{mm'}(\alpha\to\alpha')=\tfrac{1}{3}(2F_\alpha+1)(-1)^{2F_\alpha-p-p'} \times\langle 1,m-p \mid F_{\alpha'},m;F_\alpha,\bar{p}\rangle \times\langle 1,m-p \mid F_{\alpha'},m';F_\alpha,\bar{p}'\rangle\gamma(\alpha\to\alpha') , \tag{A9}$$

where $\gamma(\alpha\to\alpha')$ is the spontaneous-decay rate from state α to state α' and $\bar{p}$ is a shorthand notation for $(-p)$. (4) The field-strength parameters $G_{mm'}$ and $G'_{mm'}$ are defined by

$$G_{mm'}=\frac{(-1)^{F_b-F_c}\mid\vec{\mathscr{E}}\mid\langle F_c,m'\mid F_b,m;1,q\rangle\langle b\|D^1\|c\rangle}{2(2F_c+1)^{1/2}\hbar} =G^*_{mm'}=(-1)^{F_b-F_c}\langle F_c,m'\mid F_b,m;1,q\rangle \times[3/(2F_c+1)]^{1/2}G , \tag{A10a}$$

$$G'_{mm'}=\frac{(-1)^{F_c-F_d}|\vec{\mathscr{E}}'|\langle F_d,m'|F_c,m;1,q\rangle\langle c||D^1||d\rangle}{2(2F_d+1)^{1/2}\hbar}$$

$$=(-1)^{F_c-F_d}\langle F_d,m'|F_c,m;1,q\rangle$$

$$\times[3/(2F_d+1)]^{1/2}G' . \tag{A10b}$$

(5) The $\lambda_m(\alpha)$'s are incoherent pumping terms $[\lambda_m(\alpha)=(2F_\alpha+1)^{-1}=(2F_\alpha+1)^{-1/2}\lambda_\alpha^0]$. (6) The quantities $\eta_{\alpha\alpha'}$ are defined by

$$\eta_{bc}=\gamma_{bc}+i\beta\Delta , \tag{A11a}$$

$$\eta_{cd}=\gamma_{cd}+i\beta'\Delta' , \tag{A11b}$$

$$\eta_{bd}=\gamma_{bd}+i(\beta\Delta+\beta'\Delta') , \tag{A11c}$$

where

$$\gamma_{\alpha\beta}=\tfrac{1}{2}(\gamma_\alpha+\gamma_\beta) \tag{A12}$$

and

$$\Delta=\Omega-|\omega_{cb}| , \quad \Delta'=\Omega'-|\omega_{dc}| . \tag{A13}$$

A simple inspection of Eqs. (A7) will reveal that $\rho_{mm'}(\alpha)$ is equal to zero unless $m=m'$. This result is a direct consequence of our restricting the incident fields to be either linearly or circularly polarized according to Eq. (A5). Thus we may set

$$\rho_{mm'}(\alpha)=n_m(\alpha)\delta_{mm'} , \tag{A14}$$

where $n_m(\alpha)$ is the population of state $F_{\alpha m}$. Moreover, it is apparent that the fields only couple the triplet of levels $(F_{bm},F_{c,m+q},F_{d,m+q+q'})$. Were it not for spontaneous emission back into the levels, the problem would be reduced to a set of separate three-level problems. The terms involving $\gamma(\alpha\rightarrow\alpha')$ provide coupling between these various subsets of levels.

A *steady-state* solution to Eqs. (A7) may now be readily obtained. First, Eqs. (A7d) and (A7e) are formally solved to yield

$$\tilde{\rho}_{m,m+q}(b,c)=\eta_{bc}^{-1}\{iG_{m,m+q}[n_{m+q}(c)-n_m(b)]-iG'_{m+q,m+q+q'}\tilde{\rho}_{m,m+q+q'}(b,d)\} , \tag{A15a}$$

$$\tilde{\rho}_{m+q,m+q+q'}(c,d)=\eta_{cd}^{-1}\{iG'_{m+q,m+q+q'}[n_{m+q+q'}(d)-n_{m+q}(c)]+iG_{m,m+q}\tilde{\rho}_{m,m+q+q'}(b,d)\} . \tag{A15b}$$

When these solutions are substituted into Eqs. (A7a)—(A7c) and (A7e) one finds that $\tilde{\rho}(b,d)$ is given in terms of the populations by

$$\tilde{\rho}_{m,m+q+q'}(b,d)=(\eta_{bd}R^{bd}_{mqq'})^{-1}\{-(T^{cd}_{mqq'})^*[n_{m+q+q'}(d)-n_{m+q}(c)]+(T^{bc}_{mqq'})^*[n_{m+q}(c)-n_m(b)]\} \tag{A15c}$$

and that the populations satisfy the coupled equations

$$(A^{bb}_{mq}-B^{bb}_{mqq'})n_m(b)-(A^{bc}_{mq}-B^{bc}_{mqq'})n_{m+q}(c)-B^{bd}_{mqq'}n_{m+q+q'}(d)-\sum_p\gamma^{pp}_{mm}(c\rightarrow b)n_p(c)=\lambda_m(b) , \tag{A15d}$$

$$(A^{cc}_{mq}-B^{cc}_{mqq'})n_{m+q}(c)-(A^{cb}_{mq}-B^{cb}_{mqq'})n_m(b)-B^{cd}_{mqq'}n_{m+q+q'}(d)-\sum_{\alpha=b,d}\sum_p\gamma^{pp}_{m+q,m+q}(\alpha\rightarrow c)n_p(\alpha)=\lambda_m(c) , \tag{A15e}$$

$$(A^{dd}+B^{dd}_{mqq'})n_{m+q+q'}(d)-B^{db}_{mqq'}n_m(b)-B^{dc}_{mqq'}(c)-\sum_p\gamma^{pp}_{m+q+q',m+q+q'}(c\rightarrow d)n_p(d)=\lambda_m(d) , \tag{A15f}$$

where

$$R^{bd}_{mqq'}=\eta_{bd}+(\eta_{bc}/\eta_{cd})S_{mq}+(\eta_{cd}/\eta_{bc})S'_{mqq'} , \tag{A16a}$$

$$S_{mq}=(\eta_{bc})^{-1}(G_{m,m+q})^2 , \tag{A16b}$$

$$S'_{mqq'}=(\eta_{cd})^{-1}(G'_{m+q,m+q+q'})^2 , \tag{A16c}$$

$$S^{bc}_{mqq'}=(\eta_{bc})^{-1}G_{m,m+q}G'_{m+q,m+q+q'} , \tag{A16d}$$

$$S^{cd}_{mqq'}=(\eta_{bc}/\eta_{cd})S^{bc}_{mqq'} , \tag{A16e}$$

$$T^{bc}_{mqq'}=(\eta_{bc}/\eta^*_{bc})S^{bc}_{mqq'} , \tag{A16f}$$

$$T^{cd}_{mqq'}=(\eta_{cd}/\eta^*_{cd})S^{cd}_{mqq'} , \tag{A16g}$$

$$A^{bb}_{mq}=\gamma_b+S_{mq}+S^*_{mq} , \tag{A17a}$$

$$B^{bb}_{mqq'}=(R^{bd}_{mqq'})^{-1}S^{bc}_{mqq'}(T^{bc}_{mqq'})^*+\text{c.c.} , \tag{A17b}$$

$$A^{bc}_{mq}=S_{mq}+S^*_{mq} , \tag{A17c}$$

$$B^{bc}_{mqq'}=(R^{bd}_{mqq'})^{-1}S^{bc}_{mqq'}(T^{bc}_{mqq'}+T^{cd}_{mqq'})^*+\text{c.c.} , \tag{A17d}$$

$$B^{bd}_{mqq'}=(R^{bd}_{mqq'})^{-1}S^{bc}_{mqq'}(T^{cd}_{mqq'})^*+\text{c.c.} , \tag{A17e}$$

$$A^{cc}_{mq}=\gamma_c+S_{mq}+S^*_{mq} , \tag{A17f}$$

$$B^{cc}_{mqq'}=[-S'_{mqq'}+(R^{bd}_{mqq'})^{-1}(S^{bc}_{mqq'}+S^{cd}_{mqq'})\times(T^{bc}_{mqq'}+T^{cd}_{mqq'})^*]+\text{c.c.} , \tag{A17g}$$

$$A^{cb}_{mq}=S_{mq}+S^*_{mq} , \tag{A17h}$$

$$B^{cb}_{mqq'}=(R^{bd}_{mqq'})^{-1}(S^{bc}_{mqq'}+S^{cd}_{mqq'})+\text{c.c.} , \tag{A17i}$$

$$B^{cd}_{mqq'}=[S'_{mqq'}-(R^{bd}_{mqq'})^{-1}(S^{bc}_{mqq'}+S^{cd}_{mqq'})\times(T^{cd}_{mqq'})^*]+\text{c.c.} , \tag{A17j}$$

$$A^{dd}=\gamma_d \ , \tag{A17k}$$

$$B^{dd}_{mqq'}=[S'_{mqq'}-(R^{bd}_{mqq'})^{-1}S^{cd}_{mqq'}(T^{cd}_{mqq'})^*]+\text{c.c.} \ , \tag{A17l}$$

$$B^{db}_{mqq'}=[S'_{mqq'}-(R^{bd}_{mqq'})^{-1}S^{cd}_{mqq'} \times(T^{bc}_{mqq'}+T^{cd}_{mqq'})^*]+\text{c.c.} \ , \tag{A17m}$$

$$B^{dc}_{mqq'}=(R^{bd}_{mqq'})^{-1}S^{cd}_{mqq'}(T^{bc}_{mqq'})^*+\text{c.c.} \tag{A17n}$$

Equations (A15)—(A17) represent a solution to the steady-state problem. Since Eqs. (A15d)—(A15f) are coupled, they must still, in general, be solved numerically. However, since these equations involve level populations *only*, the maximum number of equations to be solved has been reduced to $3(2F_\alpha^{(\min)}+1)$. If the $\gamma(\alpha\rightarrow\alpha')$ terms are neglected, the equations reduce to $(2F_\alpha^{(\min)}+1)$ sets of three coupled equations for the populations $[n_m(b),n_{m+q}(c),n_{m+q+q'}(d)]$.

If the probe field is weak, the results simplify considerably. First, one can approximate $R^{bd}_{mqq'}$ by

$$R^{bd}_{mqq'}\simeq\eta_{bd}+(\eta_{bc}/\eta_{cd})S_{mq}\equiv R^{bd}_{mq} \ . \tag{A18}$$

Next, one can solve Eqs. (A15d)—(A15f) with a trial solution of the form

$$n_m(\alpha)=n_m^{(0)}(\alpha)+n_m^{(2)}(\alpha) \ , \tag{A19}$$

where $n_m^{(0)}(\alpha)$ is a solution to zero order in G' and $n_m^{(2)}(\alpha)$ is a solution to second order in G'. Substituting Eq. (A19) into (A15d)—(A15f) and using Eqs. (A16)—(A18), one finds that the $n_m^{(0)}(\alpha)$ are determined by

$$A^{bb}_{mq}n_m^{(0)}(b)-A^{bc}_{mq}n_{m+q}^{(0)}(c)-\sum_p\gamma^{pp}_{mm}(c\rightarrow b)n_p^{(0)}(c)=\lambda_m(b) \ , \tag{A20a}$$

$$A^{cc}_{mq}n_{m+q}^{(0)}(c)-A^{cb}_{mq}n_m^{(0)}(b)-\sum_{\alpha=b,d}\sum_p\gamma^{pp}_{m+q,m+q}(\alpha\rightarrow c)n_p^{(0)}(\alpha)=\lambda_m(c) \ , \tag{A20b}$$

$$A^{dd}n_{m+q+q'}^{(0)}(d)-\sum_p\gamma^{pp}_{m+q+q',m+q+q'}(c\rightarrow d)n_p^{(0)}(c)=\lambda_m(d) \ , \tag{A20c}$$

while the $n_m^{(2)}(\alpha)$ are obtained from

$$A^{bb}_{mq}n_m^{(2)}(b)-A^{bc}_{mq}n_{m+q}^{(2)}(c)-\sum_p\gamma^{pp}_{mm}(c\rightarrow b)n_p^{(2)}(c)=B^{bb}_{mqq'}n_m^{(0)}(b)-B^{bc}_{mqq'}n_{m+q}^{(0)}(c)+B^{bd}_{mqq'}n_{m+q+q'}^{(0)}(d) \ , \tag{A21a}$$

$$A^{cd}_{mq}n_{m+q}^{(2)}(c)-A^{cb}_{mq}n_m^{(2)}(b)-\sum_{\alpha=b,d}\sum_p\gamma^{pp}_{m+q,m+q}(\alpha\rightarrow c)n_p^{(2)}(\alpha)=B^{cc}_{mqq'}n_{m+q}^{(0)}(c)-B^{cb}_{mqq'}n_m^{(0)}(b)+B^{cd}_{mqq'}n_{m+q+q'}^{(0)}(d) \ , \tag{A21b}$$

$$A^{dd}n_{m+q+q'}^{(2)}(d)-\sum_p\gamma^{pp}_{m+q+q',m+q+q'}(c\rightarrow d)n_p^{(2)}(c)=-B^{dd}_{mqq'}n_{m+q+q'}^{(0)}(d)+B^{db}_{mqq'}n_m^{(0)}(b)+B^{dc}_{mqq'}n_{m+q}^{(0)}(c) \ . \tag{A21c}$$

Equations (A20) and (A21) are analytically soluble if the $\gamma(\alpha\rightarrow\alpha')$ terms are ignored. In this limit, the problem has been reduced to a set of independent analytically soluble three-level problems involving a strong pump and weak probe field. Even if the $\gamma(\alpha\rightarrow\alpha')$ terms are retained, analytic solutions are sometimes possible (see below). Equations (A20) and (A21) along with Eqs. (A15a)—(A15c) represent a solution to the three-level problem for a strong linearly or circularly polarized pump field acting on the b-c transition and a weak linearly or circularly polarized probe field acting on the c-d transition.

To end this appendix, we solve Eqs. (A20) and (A21) for the case discussed in the text. Specifically, we calculate the level d population for the upward cascade level configuration. For the upward cascade, $\gamma^{pp'}_{mm'}(c\rightarrow d)=\gamma^{pp'}_{mm'}(b\rightarrow c)=0$, and Eqs. (A20c), (A21c), and (A17k) give the upper-state population (correct to second order in $G'_{mm'}$)

$$n_{m+q+q'}(d)=\left[1-\frac{B^{dd}_{mqq'}}{\gamma_d}\right]\frac{\lambda_{m+q+q'}(d)}{\gamma_d} +B^{db}_{mqq'}n_m^{(0)}(b)+B^{dc}_{mqq'}n_{m+q}^{(0)}(c) \ , \tag{A22}$$

where $n_m^{(0)}(b)$ and $n_{m+q}^{(0)}(c)$ are solutions of Eqs. (A20). If we write

$$n_m^{(0)}(\alpha)=N_m(\alpha)+\delta n_m^{(0)}(\alpha) \ , \tag{A23}$$

where $N_m(\alpha)$ is the level population in the absence of *all* fields, Eqs. (A22) and (A20) can be recast in the form [making use of Eqs. (A17)]

$$n_{m+q+q'}(d)=N_{m+q+q'}(d)+\left\{\frac{1}{\gamma_d}\frac{(G'_{m+q,m+q+q'})^2}{[\eta_{bd}\eta_{cd}+(G_{m,m+q})^2]}\right. \times\left[\eta_{bd}[N_{m+q}(c)-N_{m+q+q'}(d)]+\left[\eta_{bd}+\frac{\gamma_c}{2\gamma_{bc}}\eta^*_{bc}\right]\delta n^{(0)}_{m+q}(c)\right]+\text{c.c.}\left.\right\} \ , \tag{A24}$$

where $N_\alpha(m)$ and $\delta n_\alpha^{(0)}(m)$ satisfy the equations

$$\left[\gamma_b+\gamma_c+\frac{\gamma_b\gamma_c|\eta_{bc}|^2}{2\gamma_{bc}(G_{m,m+q})^2}\right]\delta n_{m+q}^{(0)}(c) = -\gamma_b[N_{m+q}(c)-N_m(b)]+\sum_p \gamma_{mm}^{pp}(c\to b)\delta n_p^{(0)}(c) , \tag{A25a}$$

$$\gamma_b N_m(b)-\sum_p \gamma_{mm}^{pp}(c\to b)N_p(c)=\lambda_m(b) , \tag{A25b}$$

$$\gamma_c N_{m+q}(c)-\sum_p \gamma_{m+q,m+q}^{pp}(d\to c)N_p(d)=\lambda_{m+q}(c) , \tag{A25c}$$

$$N_{m+q+q'}(d)=\lambda_{m+q+q'}(d)/\gamma_d . \tag{A25d}$$

Equation (A24) is reminiscent of theories in which optical-pumping effects are neglected. Optical pumping modifies the weights of the line shapes arising from the various $(F_{bm},F_{c,m+q},F_{d,m+q+q'})$ subsystems, but does not significantly affect the resonance positions. If there is no incoherent pumping of levels c and d, one may reduce Eqs. (A25) to

$$N_{m+q}(c)=N_{m+q+q'}(d)=0 , \tag{A26}$$

$$\left[\gamma_b+\gamma_c+\frac{\gamma_b\gamma_c|\eta_{bc}|^2}{2\gamma_{bc}(G_{m,m+q})^2}\right]\delta n_{m+q}^{(0)}(c) =\lambda_m(b)+\sum_p \gamma_{m+q,m+q}^{pp}(c\to b)\delta n_p^{(0)}(c) . \tag{A27}$$

Equation (A27) is easily solved for either a linearly or circularly polarized pump field. The upper-state population, determined from Eqs. (A24), (A26), and (A27), was used to check computer solutions that were obtained using the irreducible tensor representation.

APPENDIX B: POSITION OF THE RESONANCES FOR ARBITRARY POLARIZATION USING A DRESSED-ATOM PICTURE

For a strong pump field of fixed detuning Δ, the number of resonance peaks which appear as the (weak) probe-field detuning Δ' is varied depends on the F values of the various levels and the polarizations of the pump field. The position of the resonances is a function of the detuning Δ and the pump-field strength. Those features are clearly seen in Figs. 4 and 6 for an $F=1\to F=2\to F=3$ system. Six resonances appear for a circularly polarized pump and four resonances for a linearly polarized pump field. In this appendix, we present a method for predicting the number and position (but *not* the strengths) of the resonances for an *arbitrary* pump-field polarization, provided that the pump field is strong ($|G|\gg$all decay rates).

A dressed-atom picture (DAP) is used to obtain these predictions. This DAP[21,26] is not the conventional one[15,16] in which the radiation fields are quantized; however, for the problem at hand (strong pump field and weak probe field incident on a three-level system) both approaches give identical results for the probe absorption line shape. The DAP is used to obtain the position of the resonances; calculation of the relative *strengths* of the resonances is somewhat more involved and is not included in this appendix.

Our calculation is similar in nature to a dressed-atom calculation for magnetically degenerate systems given by Cohen-Tannoudji and Reynaud.[65] They calculated the resonance fluorescence spectrum emitted by a "two-level" system driven by a linearly or circularly polarized pump field; we calculate the position of resonances in the probe absorption spectrum of a three-level system for an arbitrarily polarized strong pump field and a weak probe field.

We consider the upward cascade ($b\to c\to d$) between levels of angular momenta F_b, F_c, and F_d, respectively. The zero of energy is chosen such that $E_b=0$, $E_c=\hbar\omega$, and $E_d=\hbar(\omega+\omega')$. Resonance positions are obtained using a DAP by writing down the Hamiltonian for the bc subspace in a field-interaction representation. If the eigenvalues of this Hamiltonian are denoted by E_i, then possible probe absorption resonances can occur when

$$(\Delta+\Delta')=-\omega_i , \quad \omega_i=E_i/\hbar , \tag{B1}$$

where the pulse and probe detunings, Δ and Δ', are defined by

$$\Delta=\Omega-\omega=\Omega_L-\omega-\vec{k}\cdot\vec{v} ,$$
$$\Delta'=\Omega'-\omega'=\Omega'_L-\omega'-\vec{k}'\cdot\vec{v} . \tag{B2}$$

In effect, the "dressed" energy of state d is equal to $-\hbar(\Delta+\Delta')$ and resonances can occur when this dressed energy is equal to one of the dressed energies $\hbar\omega_i$ of the bc subsystem.

In the atomic rest frame, the Hamiltonian for the bc subspace may be written as $H=H_0+U$, where H_0 is the free atomic Hamiltonian (eigenvalues 0 for state $|b\rangle$ and $\hbar\omega$ for state $|c\rangle$) and U is the atom-field interaction given by [see Eqs. (A4) and (A5)]

$$U(t)=-\tfrac{1}{2}\sum_q(-1)^q D_q\epsilon_{\bar{q}}|\vec{\mathscr{E}}|e^{i\Omega t}+\text{H.c.} \tag{B3}$$

[see Eqs. (A6) for a definition of the irreducible tensor components D_q^1; the ϵ_q components of the field polarization vector are defined in an analogous manner]. If the state vector for the subsystem is expressed as

$$|\psi\rangle=\tilde{a}_b(t)|b\rangle+\tilde{a}_c(t)e^{-i\Omega t}|c\rangle \tag{B4}$$

then, in the rotating-wave approximation, the probability amplitudes $\tilde{a}_b(t)$ and $\tilde{a}_c(t)$ evolve according to

$$i\hbar\dot{\tilde{a}}_\alpha(t)=\sum_{\beta=b,c}(\tilde{H}_0+\tilde{U})_{\alpha\beta}\tilde{a}_\beta(t) , \tag{B5}$$

where matrix elements of $\tilde{H}_0$ and $\tilde{U}$ are given by

$$\langle F_b,m|\tilde{H}_0|F_b,m'\rangle=0 , \tag{B6a}$$

$$\langle F_c,m|\tilde{H}_0|F_c,m'\rangle=-\hbar\Delta\delta_{mm'} , \tag{B6b}$$

$$\langle F_b,m|\tilde{U}|F_c,m'\rangle=\langle F_c,m'|\tilde{U}|F_b,m'\rangle =-\hbar\sum_q G_{m,m+q}\epsilon_q , \tag{B6c}$$

where $G_{mm'}$ is defined by Eq. (A10a). All effects of relaxation are neglected in Eq. (B5) since the DAP is useful for predicting resonance positions only if the relaxation rates are small compared with either $|\Delta|$ or $|G|$.

Once eigenvalues of the matrix $\underline{\tilde{\omega}}$ defined by

$$\underline{\tilde{\omega}}=\underline{\tilde{H}}/\hbar=(\underline{\tilde{H}}_0+\underline{\tilde{U}})/\hbar \tag{B7}$$

are found, resonance positions can be predicted using Eq. (B1). It might seem like a formidable task to diagonalize the $(F_b+F_c+2)\times(F_b+F_c+2)$ $\underline{\tilde{\omega}}$ matrix, but certain general results can be noted.

Linear or circular polarization. If ϵ_q is chosen equal to any *one* of the values $\delta_{q,1},\delta_{q,0},\delta_{q,-1}$, the field is either circularly ($q=\pm1$) or linearly ($q=0$) polarized. In that case the $\tilde{\omega}$ matrix breaks into a number of distinct 2×2 submatrices and the diagonalization is trivial. One finds eigenvalues

$$\omega(m,q)=\tfrac{1}{2}\{-\Delta\pm[\Delta^2+4(G_{m,m+q})^2]^{1/2}\}\ , \qquad m=-F_b,\ldots,+F_b \tag{B8}$$

and resonance positions at

$$\Delta'=-\Delta-\omega(m,q) \tag{B9}$$

which is in agreement with the resonance positions determined from the denominator of Eq. (A24). It can be shown that there are always $2(F_b+F_c)$ resonances possible irrespective of whether $F_c=F_b+1$, $F_c=F_b$, or $F_c=F_b-1$. (If $F_c=F_b+1$ or $F_c=F_b$ an additional resonance, corresponding to linear absorption at $\Delta'=0$, also occurs if level c is *incoherently* pumped). For $\Delta=0$, some of these resonances may coalesce.

Elliptical polarization. By choosing

$$\epsilon_{\pm1}=\mp\frac{(1\mp\alpha)}{[2(1+\alpha^2)]^{1/2}}\ , \quad \epsilon_0=0 \tag{B10a}$$

with

$$0\le\alpha\le\infty \tag{B10b}$$

one can represent the general state of elliptical polarization for a field propagating in the z direction. In this case, one must diagonalize the full matrix $\underline{\tilde{\omega}}$. Careful inspection of the ω matrix allows one to extract at least some of the eigenvalues. For example, if $F_c=F_b+1$, $\omega_i=-\Delta$ is a double eigenvalue. Similarly, if $F_c=F_b$, $\omega_i=\Delta$ and $\omega_i=0$ are eigenvalues while, if $F_c=F_b-1$, $\omega_i=0$ is a double eigenvalue. The existence of these eigenvalues and the corresponding eigenstates imply that the *number* of possible resonances is unchanged from the case in which the pump field is linearly or circularly polarized.

To obtain the position of the resonances, one must diagonalize $\underline{\tilde{\omega}}$ [defined by Eqs. (B6) and (B7)] with ϵ_q given by Eq. (B10). Although the diagonalization must, in general, be done numerically, analytic solutions are sometimes possible. For example, if $F_b=1$, $F_c=2$, and $\Delta=0$, one finds

$$\begin{aligned}\omega_{1,2}&=\pm|G_{11}|/\sqrt{2}\ ,\\ \omega_{3,4,5,6}&=\pm(12)^{-1/2}|G_{11}|\\ &\quad\times[7\pm5(|\epsilon_1^4|+|\epsilon_{-1}^4|-\tfrac{46}{25}|\epsilon_1\epsilon_{-1}|^2)^{1/2}]^{1/2}\ .\end{aligned} \tag{B11}$$

Equation (B11) gives the positions of possible resonances for a three-level system in which a strong pump field drives an $F=1\rightarrow2$ transition and a weak field probes a coupled transition. As such, it correctly predicts the resonance positions shown in Fig. 4(e) ($\epsilon_1=1,\epsilon_{-1}=0$—circularly polarized pump field; $F_b,F_c,F_d=1,2,3$), Fig. 8 ($\epsilon_1=\epsilon_{-1}=1/\sqrt{2}$—linearly polarized pump field; $F_b,F_c,F_d=1,2,3$), and Figs. 9(a)–9(e) [$\alpha=\tan^{-1}|(\epsilon_1+\epsilon_{-1})/(\epsilon_1-\epsilon_{-1})|$—elliptically polarized pump field; $F_b,F_c,F_d=1,2,2$].

APPENDIX C: MATRIX ELEMENTS FOR TABLES I AND II

Prescriptions for calculating the elements (which are *submatrices*) of the matrices $\underline{A}$ and $\underline{B}$ appearing in Tables I and II are given as follows:

$$[A_1(b;b)]^{KK'}_{QQ'}=-\gamma_b\delta_{KK'}\delta_{QQ'}\ , \tag{C1}$$

$$\begin{aligned}[A_1(b;b,c)]^{KK'}_{QQ'}&=(-1)^{F_b-F_c+Q'-Q}\{[A_1(b;c,b)]^{KK'}_{\bar{Q}\bar{Q}'}\}^*=-\{[A_1(b,c;b)]^{K'K}_{Q'Q}\}^*\\ &=-(-1)^{F_c-F_b+Q-Q'}[A_1(c,b;b)]^{K'K}_{\bar{Q}'\bar{Q}}=iG(-1)^{F_b+F_c}\sum_q(\epsilon_{\bar{q}})^*\Lambda^{KK'\bar{q}}_{cbb}\ ,\end{aligned} \tag{C2}$$

$$[A_1(b,c)]^{KK'}_{QQ'}=\gamma^K(c\rightarrow b)\delta_{KK'}\delta_{QQ'}\ , \tag{C3}$$

$$[A_1(b,c;b,c)]^{KK'}_{QQ'}=\{[A_1(c,b;c,b)]^{KK'}_{QQ'}\}^*=-(\gamma_{bc}+i\Delta)\delta_{KK'}\delta_{QQ'}\ , \tag{C4}$$

$$\begin{aligned}[A_1(b,c;c)]^{KK'}_{QQ'}&=(-1)^{F_c-F_b+Q'-Q}\{[A_1(c,b;c)]^{KK'}_{\bar{Q}\bar{Q}'}\}^*=-\{[A_1(c;b,c)]^{K'K}_{Q'Q}\}^*\\ &=-(-1)^{F_b-F_c+Q-Q'}[A_1(c;c,b)]^{K'K}_{\bar{Q}'Q}=-iG(-1)^{F_b+F_c+K'-K+1}\sum_q(-1)^q\epsilon_{\bar{q}}\Lambda^{KK'q}_{cbc}\ ,\end{aligned} \tag{C5}$$

$$[A_1(c;c)]^{KK'}_{QQ'}=-\gamma_c\delta_{KK'}\delta_{QQ'}\ , \tag{C6}$$

$$[A_2(c,d;c,d)]^{KK'}_{QQ'}=\{[A_2(d,c;d,c)]^{KK'}_{QQ'}\}^*=-(\gamma_{cd}+i\Delta')\delta_{KK'}\delta_{QQ'}\ , \tag{C7}$$

$$[A_2(c,d;b,d)]^{KK'}_{QQ'}=(-1)^{F_b-F_c+Q'-Q}\{[A_2(d,c;d,b)]^{KK'}_{\bar{Q}\bar{Q}'}\}^*$$
$$=-\{[A_2(b,d;c,d)]^{K'K}_{Q'Q}\}^*=-(-1)^{F_c-F_b+Q-Q'}\{[A_2(d,b;d,c)]^{K'K}_{\bar{Q}'\bar{Q}}\}^*$$
$$=-iG(-1)^{F_b+F_d+K'-K+1}\sum_{\bar{q}}(\epsilon_{\bar{q}})^*\Lambda^{KK'\bar{q}}_{bcd}\,, \tag{C8}$$

$$[A_2(b,d;b,d)]^{KK'}_{QQ'}=\{[A_2(d,b;d,b)]^{KK'}_{QQ'}\}^*=-[\gamma_{bd}+i(\Delta+\Delta')]\delta_{KK'}\delta_{QQ'}\,, \tag{C9}$$

$$[A_3(d;d)]^{KK'}_{QQ'}=-\gamma_d\delta_{KK'}\delta_{QQ'}\,, \tag{C10}$$

$$[B_1(b,c;b,d)]^{KK'}_{QQ'}=-(-1)^{F_c-F_d+Q'-Q}\{[B_1(c,b;d,b)]^{KK'}_{\bar{Q}\bar{Q}'}\}^*$$
$$=\{[B_2(b,d;b,c)]^{K'K}_{Q'Q}\}^*=-(-1)^{F_d-F_c+Q-Q'}[B_2(d,b;c,b)]^{K'K}_{\bar{Q}'\bar{Q}}$$
$$=(-1)^{F_b+F_d}\sum_{\bar{q}}(\epsilon'_{\bar{q}})^*\Lambda^{KK'\bar{q}}_{dcb}\,, \tag{C11}$$

$$[B_1(c;c,d)]^{KK'}_{QQ'}=-(-1)^{F_c-F_d+Q'-Q}\{[B_1(c;d,c)]^{KK'}_{\bar{Q}\bar{Q}'}\}^*$$
$$=(-1)^{F_c+F_d}\sum_{\bar{q}}(\epsilon'_{\bar{q}})^*\{\Lambda^{KK'\bar{q}}_{dcc}-[\gamma^K(d\to c)/\gamma_d](-1)^{1+K'-K}\Lambda^{KK'\bar{q}}_{cdd}\}\,, \tag{C12}$$

$$[B_2(c,d;c)]^{KK'}_{QQ'}=-(-1)^{F_d-F_c+Q'-Q}\{[B_2(d,c;c)]^{KK'}_{\bar{Q}\bar{Q}'}\}^*=(-1)^{F_c+F_d}\sum_{\bar{q}}(-1)^q\epsilon'_{\bar{q}}\Lambda^{KK'q}_{cdc}\,, \tag{C13}$$

$$[B_3(c,d;d)]^{KK'}_{QQ'}=-(-1)^{F_d-F_c+Q'-Q}\{[B_3(d,c;d)]^{KK'}_{\bar{Q}\bar{Q}'}\}^*$$
$$=-(-1)^{1+K'-K+F_c+F_d}\sum_{\bar{q}}(-1)^q\epsilon'_{\bar{q}}\Lambda^{KK'q}_{dcd}\,. \tag{C14}$$

---

*Present address: Naval Ocean Research and Development Activity, Code 320, National Space Technology Laboratories Station, MS 39529.

[1]An excellent bibliography may be found in Chap. 10 of the book by Demtröder [W. Demtröder, *Laser Spectroscopy* (Springer, Berlin, 1981)]. Additional sources of general references are *Laser Spectroscopy III,* edited by J. L. Hall and J. L. Carlsten (Springer, New York, 1977); *Laser Spectroscopy IV,* edited by H. Walther and K. W. Rothe (Springer, Berlin, 1979); *Laser Spectroscopy V,* edited by A. R. W. McKellar, T. Oka, and B. P. Stoicheff (Springer, Berlin, 1981); *High Resolution Laser Spectroscopy,* edited by K. Shimoda (Springer, New York, 1976); *Laser Spectroscopy of Atoms and Molecules,* edited by H. Walther (Springer, New York, 1976); V. S. Letokhov and V. P. Chebotaev, *Nonlinear Laser Spectroscopy* (Springer, New York, 1977); *Frontiers in Laser Spectroscopy,* edited by R. Balian, S. Haroche, and S. Liberman (North-Holland, Amsterdam, 1977). Listed below are some selected references in this field.

[2]G. E. Notkin, S. G. Rautian, and A. A. Feoktistov, Zh. Eksp. Teor. Fiz. 52, 1673 (1967) [Sov. Phys.—JETP 25, 1112 (1967)].

[3]M. S. Feld and A. Javan, Phys. Rev. 177, 540 (1969).

[4]T. W. Hänsch and P. E. Toschek, Z. Phys. 236, 213 (1970).

[5]S. Haroche and F. Hartmann, Phys. Rev. A 6, 1280 (1972).

[6]N. Skribanowitz, M. J. Kelly, and M. S. Feld, Phys. Rev. A 6, 2302 (1972).

[7]I. M. Beterov and V. P. Chebotaev, Prog. Quantum Electron. 3, 1 (1974), and references therein.

[8]R. M. Whitley and C. R. Stroud, Phys. Rev. A 14, 1498 (1976).

[9]R. Salomaa and S. Stenholm, J. Phys. B 8, 1795 (1975); 9, 1221 (1976).

[10]R. Salomaa, J. Phys. B 10, 3005 (1977).

[11]R. Salomaa, Phys. Scr. 15, 251 (1977).

[12]C. Delsart and J. C. Keller, J. Phys. (Paris) 39, 350 (1978).

[13]P. R. Berman, P. F. Liao, and J. E. Bjorkholm, Phys. Rev. A 20, 2389 (1979).

[14]V. P. Kaftandjian, C. Delsart, and J. C. Keller, Phys. Rev. A 23, 1365 (1981); V. P. Kaftandjian, doctoral thesis, University of Provence, France, 1977 (unpublished).

[15]C. Cohen-Tannoudji and S. Reynaud, J. Phys. B 10, 345 (1977); 10, 365 (1977).

[16]C. Cohen-Tannoudji and S. Reynaud, J. Phys. B 10, 2311 (1977).

[17]S. Reynaud, thesis of third cycle, University of Paris, 1977 (unpublished).

[18]F. Hoffbeck, thesis of third cycle, University of Paris, 1978 (unpublished).

[19]E. Arimondo and P. Glorieux, Phys. Rev. A 19, 1067 (1979).

[20]M. Himbert, thesis of third cycle, University of Paris, 1980 (unpublished).

[21]P. R. Berman and R. Salomaa, Phys. Rev. A 25, 2667 (1982).

[22]H. W. Galbraith, M. Dubs, and J. I. Steinfeld, Phys. Rev. A 26, 1528 (1982).

[23]A. Ben Reuven and L. Klein, Phys. Rev. A 4, 753 (1971).

[24]L. Klein, M. Giraud, and A. Ben Reuven, Phys. Rev. A 10, 682 (1974).

[25]Y. Rabin and A. Ben Reuven, J. Phys. B 13, 2011 (1980).

[26]G. Nienhuis, J. Phys. B 14, 3117 (1981).

[27]D. Grischkowsky, M. M. T. Loy, and P. F. Liao, Phys. Rev. A 12, 2514 (1975).

[28]R. G. Brewer and E. L. Hahn, Phys. Rev. A 11, 1641 (1975).

[29]D. Grischkowsky, Phys. Rev. A 14, 802 (1976).

[30]M. Sargent III and P. Horwitz, Phys. Rev. A 13, 1962 (1976).

[31]D. P. Hodginson and J. S. Briggs, Opt. Commun. 22, 45 (1977).
[32]J. R. Ackerhalt and B. W. Shore, Phys. Rev. A 16, 277 (1977); B. W. Shore and J. R. Ackerhalt, *ibid.* 15, 1640 (1977).
[33]M. Ducloy, J. R. R. Leite, and M. S. Feld, Phys. Rev. A 17, 623 (1978); J. R. R. Leite, R. L. Sheffield, M. Ducloy, R. D. Sharma, and M. S. Feld, *ibid.* 14, 1151 (1976).
[34]M. P. Silverman, S. Haroche, and M. Gross, Phys. Rev. A 18, 1507 (1978); 18, 1517 (1978).
[35]T. W. Mossberg, R. Kachru, S. R. Hartmann, and A. M. Flusberg, Phys. Rev. A 20, 1976 (1979), and references therein.
[36]A. Schenzle and R. G. Brewer, Phys. Rev. A 14, 1756 (1976); Phys. Rep. 43, 455 (1978).
[37]L. Kancheva, D. Pushkarov, and S. Rashev, J. Phys. B 14, 573 (1981).
[38]A. I. Alekseev and A. M. Basharov, J. Phys. B 15, 4269 (1982).
[39]For a review of line shapes in laser experiments, see R. Vetter and P. R. Berman, Comments At. Mol. Phys. 10, 69 (1981).
[40]T. Hänsch, R. Keil, A. Schabert, Ch. Schmelzer, and P. Toschek, Z. Phys. 226, 293 (1969).
[41]J. E. Bjorkholm and P. F. Liao, Phys. Rev. Lett. 33, 128 (1974).
[42]A. Schabert, R. Keil, and P. E. Toschek, Opt. Commun. 13, 265 (1975).
[43]C. Delsart and J. C. Keller, Opt. Commun. 15, 91 (1975); 16, 338 (1976).
[44]R. P. Hackel and S. Ezekiel, in *Laser Spectroscopy IV,* edited by H. Walther and K. W. Rothe (Springer, Berlin, 1979), pp. 88—95 and references therein.
[45]M. Himbert, S. Reynaud, J. Dupont-Roc, and C. Cohen-Tannoudji, Opt. Commun. 30, 184 (1979).
[46]Ph. Cahuzac, J. L. LeGouët, and R. Vetter, Appl. Phys. (Germany) 20, 83 (1979).
[47]U. Fano, Rev. Mod. Phys. 29, 74 (1957).
[48]U. Fano, Phys. Rev. 131, 259 (1963).
[49]K. Blum, *Density Matrix Theory and Applications* (Plenum, New York, 1981), Chap. 1.
[50]C. Bottcher and C. Feuillade, Chem. Phys. 26, 319 (1977).
[51]J. C. McGurk, T. G. Schmalz, and W. H. Flygare, Adv. Chem. Phys. 25, 1 (1974).
[52]J. G. Baker, in *Modern Aspects of Microwave Spectroscopy,* edited by G. W. Chantry (Academic, New York, 1979).
[53]M. Sargent, M. O. Scully, and W. E. Lamb, *Laser Physics* (Addison-Wesley, New York, 1974), Chap. 7.
[54]A. Omont, *Progress in Quantum Electronics* (Pergamon, Oxford, 1977), Vol. 5, p. 69; see also W. Happer, *Progress in Quantum Electronics* (Pergamon, Oxford, 1970), Vol. 1, Pt. 2.
[55]C. Bottcher and C. Feuillade, Chem. Phys. 54, 227 (1981).
[56]C. Feuillade and C. Bottcher, Chem. Phys. 62, 671 (1981).
[57]C. P. Slichter, *Principles of Magnetic Resonance,* 2nd ed. (Springer, Berlin, 1978), pp. 30—32 and p. 241.
[58]I. I. Sobelman, *Atomic Spectra and Radiative Transitions* (Springer, Berlin, 1979), Chap. 9.
[59]M. Dumont, J. Phys. (Paris) 33, 971 (1972).
[60]M. Ducloy, Phys. Rev. A 8, 1844 (1973).
[61]J. E. Bjorkholm, P. F. Liao, and A. Wokaun, Phys. Rev. A 26, 2643 (1982).
[62]J. R. Morris and B. W. Shore, Phys. Rev. A 27, 906 (1983).
[63]The irreducible tensor components ϵ_q and ϵ'_q of the field polarization vectors do not appear in Eq. (A5). Since only *one* of each of these components contributes on each transition, we have arbitrarily set that component equal to unity. In effect, this corresponds to a choice of phase for the field amplitudes. Equations (A7) can be generalized to fields of arbitrary polarization by making the replacements

$$X_{m,m+Q} \rightarrow [P_B(Q)]X_{m,m+Q} ,$$

$$X_{m',m'+Q} \rightarrow [P_B(Q)]^* X_{m',m'+Q} ,$$

$$X_{m-Q,m} \rightarrow [P_B(Q)]^* X_{m-Q,m} ,$$

$$X_{m'-Q,m'} \rightarrow [P_B(Q)]X_{m'-Q,m'} ,$$

where the set (X,P,B,Q) is equal to (G,ϵ,β,q) or (G',ϵ',β',q') and $P_1(Q)=P_Q$, $P_{-1}(Q)=(-1)^Q(P_{-Q})^*$, and summing over q and q'.
[64]The terms containing G and G' in Eqs. (A7) are written specifically for the case $\beta=\beta'=1$. If $\beta=-1$, one must multiply any term containing G by $(-1)^q$ and also change all values of q appearing in those terms to $-q$. Similarly, if $\beta'=-1$, one must multiply any term containing G' by $(-1)^{q'}$ and also change all values of q' appearing in those terms to $-q'$. This result follows from Ref. 63 when one chooses $\epsilon_q=\delta_{qq_0}$ and $\epsilon_{q'}=\delta_{q'q'_0}$.
[65]C. Cohen-Tannoudji and S. Reynaud, J. Phys. (Paris) Lett. 38, L173 (1977).